

IMPERIAL COLLEGE LONDON

Department of Earth Science and Engineering

Centre for Petroleum Studies

Interpretation of polymer solution injection fall-off tests

By

Ajana Laoroongroj

**A report submitted in partial fulfillment of the requirements for
the MSc and/or the DIC.**

September 2011

DECLARATION OF OWN WORK

I declare that this thesis

“Interpretation of polymer solution injection fall-off tests”

is entirely my own work and that where any material could be construed as the work of others, it is fully cited and referenced, and/or with appropriate acknowledgement given.

Signature:

Name of student: **Ajana Laoroongroj**

Name of supervisor: **Alain Gringarten**

Abstract

Polymer injection to increase oil recovery from medium viscous or heavy oils has been successful and is currently attracting a lot of attention.

One of the key design parameters for such projects is the in-situ viscosity of polymer solutions to optimize the displacement efficiency while minimizing costs for the polymers. The viscosity of polymer solutions for different polymer concentrations can be measured at the surface; however, the viscosity of such solutions in the reservoir is difficult to estimate. The reason is that the viscosity in the reservoir depends on the degradation of the polymers during the injection process and the shear rate in the reservoir.

In this study, the in-situ polymer properties are investigated based on a water injection fall-off test performed in an Austrian reservoir. The fall-off test was analyzed and the determined reservoir parameters used for subsequent polymer injection simulations. The results of the simulations show that pressure transient analysis of a series of fall-off tests gives useful information concerning polymer augmented waterfloods such as the in-situ viscosity and the location of the polymer front. Even for Non-Newtonian fluid behavior – as observed for polymer solutions – an average viscosity and location of the front can be inferred from pressure transient analysis.

Acknowledgements

First of all, I would like to express my deepest and sincere gratitude to my project advisors, Professor Alain Gringarten and Torsten Clemens, for their continuous supervision throughout this study. They always spent their time in giving me advice and teaching me how to express my ideas to the study. Their valuable guidance was very useful in completing this study. Besides my advisors, I would like to express my gratefulness to Mr. Markus Zechner. Without his corporation I could not have gotten such relevant data.

Lastly I would like to thank my family: my parents and my brothers. I could not have accomplished this project without a great support and encouragement to pursue my interests. Also I would like to thank all Lecturers and Department Staffs for good administrations, and all friends in supporting me.

Table of Contents

DECLARATION OF OWN WORK	ii
Abstract.....	iii
Acknowledgements.....	iv
Lists of Tables.....	vi
Lists of Figures	vii
Abstract.....	1
Introduction.....	1
Rheology of Polymer Solutions	2
Radial-composite flow model	3
Field Introduction 8 TH Horizon, Matzen Field, Austria.....	5
Interpretation of polymer solution injection fall-off tests without shear-thinning effect	8
Interpretation of polymer solution injection fall-off tests with shear-thinning effect	12
Summary and Conclusions.....	14
Nomenclature.....	14
Acknowledgements.....	15
References.....	15
Appendix A: Milestones in interpretation of polymer solution injection fall-off test study	A-1
Appendix B: Critical Literature Review	B-1
Appendix C: ECLIPSE Reservoir Modeling.....	C-1
Appendix D: Sapphire program	D-1
Appendix E: Rheology of Polymer Solutions	E-1

Lists of Tables

Table 1: Well and reservoir parameters of Schönkirchen C 1	5
Table 2: Matching parameters of the two water injection fall-off tests of the well Schönkirchen C 1	7
Table 3: Reservoir and fluid properties in reservoir simulation	8
Table 4: Polymer Solution Viscosity at Different Polymer Concentration	8
Table 5: Injection time effect of composite system for simulated fall-off tests	9
Table 6: Heterogeneity effect of composite system for simulated fall-off tests	10
Table 7: Effect of polymer concentration	11
Table 8: Permeability reduction effect of composite system for simulated fall-off tests	12
Table 9: Effect of polymer concentration in shear-thinning behavior	14

Lists of Figures

Figure 1: Two-region, radial composite reservoir	3
Figure 2: Log-log plot of the two water injection fall-off test of the well Schönkirchen C 1	6
Figure 3 Log-log plot, semi-log plot and history plot of the 1 st fall-off test	6
Figure 4: Log-log plot, semi-log plot and history plot of the 2 nd fall-off test.....	6
Figure 5: History matching of the water injection fall-off tests for homogeneous and heterogeneous reservoirs	7
Figure 6: Pressure response as a function of injection period	9
Figure 7: Log-log bottom-hole pressure as a function of injection time	9
Figure 8: Log-log bottom-hole pressure for one-layer and five-layer reservoirs	10
Figure 9: Pressure response as a function of polymer concentration	11
Figure 10: Log-log plot of simulated bottom-hole pressure fall-off test as a function of polymer concentration.....	11
Figure 11: Effect of permeability reduction	12
Figure 12: Lab measurement of polymer solution of FP 3630.....	12
Figure 13: the Correlation between Polymer Solution Viscosity and Darcy velocity Used in Reservoir Simulation	12
Figure 14: Apparent viscosity as a function of well distance and polymer concentration	13
Figure 15: Bottom-hole reservoir pressure with and without shear-thinning effect at 0.75 kg/m ³ polymer concentration.....	13
Figure 16: Pressure response with shear thinning effect as a function of polymer concentration.....	13
Figure 17: Log-log plot of simulated bottom-hole pressure fall-off test with Shear thinning fluids as a function of polymer concentration.....	13
Figure 18: Polymer viscosity with shear thinning behavior at instant shut-in for 0.75 kg/m ³ polymer concentration.....	14
Figure C- 1: Radial grid geometry for 1 km external boundary	C-1
Figure C- 2: Radial grid geometry for 2 km external boundary	C-1
Figure C- 3: Polymer viscosity at C = 0.25 kg/m ³ without shear thinning at instant shut in.....	C-1
Figure C- 4: Polymer viscosity at C = 0.25 kg/m ³ without shear thinning behavior for ten days after shut in	C-1
Figure C- 5: Polymer viscosity at C = 0.75 kg/m ³ without shear thinning at instant shut in.....	C-2
Figure C- 6: Polymer viscosity at C = 0.75 kg/m ³ without shear thinning behavior for ten days after shut in	C-2
Figure C- 7: Polymer viscosity at C = 1.25 kg/m ³ without shear thinning at instant shut in.....	C-2
Figure C- 8: Polymer viscosity at C = 1.25 kg/m ³ without shear thinning behavior for ten days after shut in	C-2
Figure C- 9: Polymer viscosity at C = 0.75 kg/m ³ with shear thinning behavior for two days before shut in.....	C-2
Figure C- 10: Polymer viscosity at C = 0.75 kg/m ³ with shear thinning behavior for one day before shut in	C-2
Figure C- 11: Polymer viscosity at C = 0.75 kg/m ³ with shear thinning behavior at instant shut-in	C-3
Figure C- 12: Polymer viscosity at C = 0.75 kg/m ³ with shear thinning behavior for one day after shut in	C-3
Figure C- 13: Polymer viscosity at C = 0.75 kg/m ³ with shear thinning behavior for two days after shut in	C-3
Figure C- 14: Polymer viscosity at C = 0.75 kg/m ³ with shear thinning behavior for ten days after shut in	C-3
Figure D- 1: Log-log, semi-log and history plot for 6 days polymer injection and R = 20 m.....	D-1
Figure D- 2: Log-log, semi-log and history plot for 23 days polymer injection and R = 40 m.....	D-2
Figure D- 3: Log-log, semi-log and history plot for 51 days polymer injection and R = 60 m.....	D-2
Figure D- 4: Log-log, semi-log and history plot for 90 days polymer injection and R = 80 m.....	D-3
Figure D- 5: Log-log, semi-log and history plot for 23 days polymer injection in the five layers of constant 550 md permeability	D-3
Figure D- 6: Log-log, semi-log and history plot for 23 days polymer injection in the five layers of 330, 440, 550, 660 and 770 md permeability	D-4
Figure D- 7: Log-log, semi-log and history plot for 23 days polymer injection in the five layers of 100, 400, 550, 600 and 1000 md permeability	D-4
Figure D- 8: Log-log, semi-log and history plot for 23 days polymer injection for RRF = 1.0	D-5
Figure D- 9: Log-log, semi-log and history plot for 23 days polymer injection for RRF = 1.5	D-5
Figure D- 10: Log-log, semi-log and history plot for 23 days polymer injection for RRF = 2.0	D-6
Figure D- 11: Log-log, semi-log and history plot for 51 days polymer injection with C = 0.25 kg/m ³	D-6
Figure D- 12: Log-log, semi-log and history plot for 51 days polymer injection with C = 0.75 kg/m ³	D-7
Figure D- 13: Log-log, semi-log and history plot for 51 days polymer injection with C = 1.25 kg/m ³	D-7
Figure D- 14: Log-log, semi-log and history plot for 51 days shear-thinning polymer injection with C = 0.5 kg/m ³	D-8
Figure D- 15: Log-log, semi-log and history plot for 51 days shear-thinning polymer injection with C = 0.75 kg/m ³	D-8
Figure D- 16: Log-log, semi-log and history plot for 51 days shear-thinning polymer injection with C = 1.0 kg/m ³	D-9
Figure E- 1: Log-log plot of polymer shear rate and viscosity.....	E-1

MSc in Petroleum Engineering 2010-2011

Thesis title: Interpretation of polymer solution injection fall-off tests

Student name: **Ajana Laoroongroj**

Imperial College supervisor: **Alain Gringarten**

Company supervisor: **Torsten Clemens (OMV Exploration & Production GmbH)**

Abstract

Polymer injection to increase oil recovery from medium viscous or heavy oils has been successful and is currently attracting much of attention.

One of the key design parameters for such projects is the in-situ viscosity of polymer solutions to optimize the displacement efficiency while minimizing costs for the polymers. The viscosity of polymer solutions for different polymer concentrations can be measured at the surface; however, the viscosity of such solutions in the reservoir is difficult to estimate. The reason is that the viscosity in the reservoir depends on the degradation of the polymers during the injection process and the shear rate in the reservoir.

In this study, the in-situ polymer properties are investigated based on a water injection fall-off test performed in an Austrian reservoir. The fall-off test was analyzed and the determined reservoir parameters used for subsequent polymer injection simulations. The results of the simulations show that pressure transient analysis of a series of fall-off tests gives useful information concerning polymer augmented waterfloods such as the in-situ viscosity and the location of the polymer front. Even for Non-Newtonian fluid behavior – as observed for polymer solutions – an average viscosity and location of the front can be inferred from pressure transient analysis.

Introduction

Recently, non-Newtonian fluids, such as polymer solutions, have been used for enhanced oil recovery. In general, these polymer solutions are injected into reservoirs to reduce the mobility of aqueous phase and increase oil sweep efficiency by two mechanisms – their high viscosity characteristic and the reduction of the aqueous phase permeability.

Some enhanced oil recovery projects by injection of polymers are successful; others underperformed or fail (Clark 1993, Han 2006, Chang et al. 2006, Du 2004). Therefore, it is crucial to study the flow of polymer solutions in porous media.

The concept of mobility ratio was first introduced by Muskat (1937). Its definition is the mobility of the displacing fluid divided by the mobility of the displaced phase ahead of the front. The mobility ratio is one of the important factors determining the efficiency of the water flooding and polymer augmented water flooding projects. The displacement efficiency of water flooding viscous oils is improved by increasing the displacing fluid viscosity. The lower the mobility ratio, the more efficient the displacement. In addition, some researchers reported that the apparent polymer viscosity is related to the permeability because of high polymer retention in low permeability reservoirs. (W. B. Gogarty 1967, Szabo 1975).

Several studies of a non-Newtonian rheology in porous media have been presented since 1950. The rheological behavior of the polymer viscosity is expressed as the apparent viscosity. At low shear rate, the apparent viscosity is limited by the maximum value (McKinley 1966, W. Gogarty 1967, Sadowski 1965). For a range of shear rate, the apparent viscosity is decreasing with increasing shear rate called pseudoplastic or shear-thinning behavior (Christopher 1965, W. B. Gogarty 1967, Smith 1970). At high shear rate, the apparent viscosity approaches the minimum value (Pye 1964, Dauben 1967, Marshall 1967).

The polymer viscosity can be measured at the surface, but the apparent viscosity of polymer solution at reservoir condition is unknown due to shear-thinning characteristic by high shear rate near wellbore and degradation of the polymers during the injection process. The correct apparent viscosity is needed to design a stable polymer injection by adjusting polymer concentration.

With the characteristic of the mobility contrast (k/μ) between inner and outer zone, transient pressure analysis can be applied to estimate both the apparent viscosity and the location of the polymer front in the reservoir.

In this study the flow of a Newtonian fluid - for which the apparent viscosity is constant with shear rate - and the flow of Non-Newtonian fluid - for which the viscosity varies with shear rate - is considered.

In most reservoirs water injection is initiated in the early stage of field development. An injectivity test can give information about reservoir properties such as permeability and near well-bore damage. If properly analyzed, the provided information can give an insight for the design of polymer flooding to enhance oil recovery. In the particular reservoir investigated here, the permeability and skin parameters are determined based on a water injection fall-off test. By knowing the reservoir properties and performing polymer injection fall-off tests, the polymer front and apparent viscosity can be estimated using subsequent fall-off tests during polymer flooding. A composite reservoir model is used to analyze well-tests for two or more region reservoirs which have their own rock and fluid properties.

The paper is organized as follows: in the following paragraph, the rheology of polymer solutions is described. Then, radial composite models for pressure transient analysis are covered. These models were used to investigate the in-situ polymer viscosity and position of the polymer front. Afterwards, the oil field in which polymer flooding is planned is introduced and a water injection fall-off test is analyzed. Then, the derived reservoir parameters were used to construct a radial finite difference model. This model was used to simulate the planned polymer injection and fall-off tests. The fall-off tests with the simulated polymer injection were then analyzed using pressure transient analysis. The results from the pressure transient analysis were then compared with the simulation model for injection of polymer solutions for which Newtonian and Non-Newtonian behavior was assumed.

Rheology of Polymer Solutions

Polymer rheology has been investigated to describe the flow behavior in porous media (Marshall 1967, and McKinley 1966). A flow equation is taking into account the effect of tortuosity on shear rate and shear stress. This behavior is determined by a core flow experiment for which the pressure drop as a function of flow rate and the viscosity of the fluid is recorded (Christopher 1965).

While Newtonian fluids such as brine exhibit a linear relationship between the shear stress, and the shear rate, aqueous polymer solutions do not show such linear relationship. The viscosity of such solutions decreases at increasing shear and flow rate, the so-called shear-thinning effect. This effect disappears at lower shear rates and then the polymer solution behaves Newtonian flow in porous media (Wang 1979).

The flow behavior of polymer solution has to take account of non-Newtonian fluids. Many non-Newtonian fluids follow the power-law models (Teeuw 1980). This describes the behavior of shear-thinning and shear-thickening polymer solutions.

$$\mu_{app} = K\gamma^{n-1} \quad (1)$$

Where μ_{app} = apparent viscosity, cP
 K = consistency index, cP.sⁿ⁻¹
 n = power law exponent
 γ = Shear rate, s⁻¹

For a Newtonian fluid, n is equal to 1 and the viscosity is constant to K . For pseudoplastic fluids, n is between zero and one and negative slope is indicated from a graph of $\log\mu_{app}$ and $\log\gamma$. If n is more than one, the fluid is dilatants or shear thickening fluids which the apparent viscosity increases with the shear rate.

To allow for the shear-thinning characteristics Darcy's equation must be adapted. The shear rate is converted into a superficial flow rate (Darcy velocity) in the porous media. The derivation of this equation is based on the flow in a cylindrical tube or capillary. The flow of non-Newtonian fluids through capillary tube is proposed by Teeuw 1980.

$$\gamma = \left(\frac{3n+1}{n}\right) \frac{u}{\sqrt{8k\phi}} \quad (2)$$

Where u = superficial flow rate, m/s
 k = permeability, m²
 ϕ = porosity, fraction

Polymer options in reservoir simulation demand power-law parameters as input for the calculation of injection pressures. The model targets the shear thinning of polymer that the polymer viscosity reduces at higher flow rates. It assumes that shear rate is

proportional to the flow viscosity and the apparent viscosity is a function of Darcy velocity.

Radial-composite flow model

Polymer injection into a reservoir results in a mobility discontinuity in a near wellbore region due to the different reservoir properties between an inner and an outer region (Bixel 1967). Consequently, radial composite model is used to analysis the two-region reservoir. The model consists of an inner cylindrical region surrounded by an outer different property region as shown in Figure 1. The distance R is the front or discontinuity radius, an important parameter inferred by well tests in composite reservoirs.

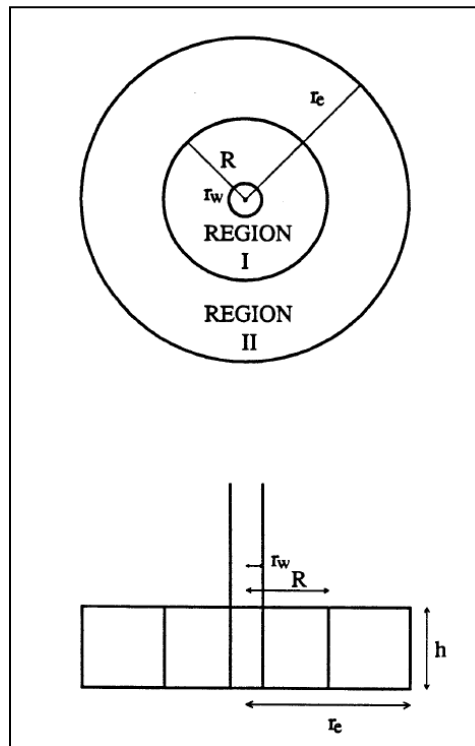


Figure 1: Two-region, radial composite reservoir

Van Poolen (1964) used the concept of drainage radius, and related it to a deviation time from the semi-log straight line corresponding to the two-phase inner region mobility. Later, van Poolen (1965) located the burning front radius in an in-situ combustion project using the deviation time method for pressure fall-off data from in-situ combustion projects.

$$R = \sqrt{\frac{0.25k_i t_e}{(\phi c_t \mu)_i t_{De}}} \tag{3}$$

where $(k, \phi, c_t, \mu)_i$ are the permeability, porosity, total compressibility and viscosity in inner region. t_e and t_{De} are the deviation time and dimensionless deviation time based on the front radius. And R is the radius of the discontinuity. However, it is quite difficult to obtain an accurate deviation if there is a small mobility contrast.

Wattenbarger and Ramey (1970) modeled a skin region as the two-region composite reservoir using finite-difference techniques. The mobility ratio, M, is governed as follows.

$$M = \frac{\left(\frac{k}{\mu}\right)_i}{\left(\frac{k}{\mu}\right)_o} \tag{4}$$

Odeh (1969) observed that pressure data measured at a shut-in well in a composite reservoir show a semi-log straight line, a transition, and followed by a second semi-log straight line corresponding to the inner region mobility, transition and the outer region mobility respectively. He proposed a correlation between the dimensionless discontinuity radius, R_D , and the dimensionless intersection time, t_{DX} , for equal storativity in both regions as:

$$R_D^2 = \frac{2.25t_{DX}}{M} \quad (5)$$

$$R_D = \frac{R}{r_w} \quad (6)$$

$$t_{DX} = \frac{0.00264k_i t_x}{(\phi c_t \mu)_i r_w^2} \quad (7)$$

where the storativity ratio, S, is governed by equation as:

$$S = \frac{(\phi c_t \mu)_i}{(\phi c_t \mu)_o} \quad (8)$$

Ramey (1970) presented a more general equation relating R_D and t_{DX} as:

$$R_D^2 = \frac{2.2458t_{DX}}{D^{(M-1)}} \quad (9)$$

where the diffusivity ratio, D, is governed by equation as:

$$D = \frac{\left(\frac{k}{\phi c_t \mu}\right)_i}{\left(\frac{k}{\phi c_t \mu}\right)_o} \quad (10)$$

The intersection time method relies on the two semi-log straight lines. The first semi-log straight line will be obscured by wellbore storage, while the second semi-log straight line has a dominant boundary effect. Hence, the intersection method sometimes is inapplicable.

Eggemchwilr et al. (1979) observed the mobility and storativity contrast between two regions and developed a pseudosteady state method to calculate inner swept volume for composite reservoirs. After the first semi-log straight line, a pseudosteady Cartesian is developed and the inner swept volume, V_s , is calculated by the slope, m_c , of the Cartesian line expressed in field units as:

$$m_c = \frac{5.615qB}{V_s c_t} \quad (11)$$

Where q is the flow rate, B is the formation volume factor.

And the volume of inner zone is given by:

$$V_s = \pi R^2 h \phi_i \quad (12)$$

$$R = \sqrt{\frac{V_s}{\pi h \phi_i}} \quad (13)$$

Type-curve matching is another method for calculating the inner region mobility (Brown 1985, Olarewaju 1987).

$$\frac{k}{\mu_1} = \frac{qB}{h} \left(\frac{\frac{dp_{wD}}{d \log t_D}}{\frac{d \Delta p_{wD}}{d \log \Delta t_D}} \right)_{Match} \quad (14)$$

where p_{wD} and Δp_{wD} are dimensionless wellbore pressure drop and wellbore pressure drop. h is the formation thickness. The front radius is estimated by the time match if the inner region properties are known.

$$R = \sqrt{\frac{0.25k_i}{(\phi c_t \mu)_i} \left(\frac{\Delta t}{t_{De}} \right)_{Match}} \quad (15)$$

where t_{De} is dimensionless time corresponding to the front radius R.

Composite reservoir models have extensively applied to enhanced recovery process. Van pollen (1964) used a deviation time method to find the inner region mobility for an in-situ combustion project. Walsh et al. (1981), Messner and Williams (1982a and b) Onyekonwu et al. (1984 and 1986), and Da Prat et al. (1985) applied the pseudosteady state method to well tests for in-situ combustion and steam injection projects. Also, Horne et al. (1980) analyzed geothermal well test data using the pseudosteady state method. MacAllister (1987) used the pseudosteady state method to analyze well tests in CO₂ flooding projects.

Transient pressure behavior of composite reservoirs for in-situ combustion, steam injection and CO₂ flooding has been discussed; however, transient pressure behavior of composite reservoir for polymer flooding has attracted little attraction. Therefore, this study investigates polymer solution injection fall-off tests by using two-region radial composite reservoir. The objectives of this study are to interpret the pressure behavior for well tests in both homogeneous and heterogeneous composite reservoirs and to analyze well test reports using composite reservoir model to estimate a front radius of swept volume and apparent viscosity. The injected polymer solution behaves as a Newtonian and pseudoplastic Non-Newtonian fluid.

Field Introduction 8 TH Horizon, Matzen Field, Austria

The 8 TH horizon of the Matzen Field is located about 20 km northeast of Vienna in the Vienna Basin. Its first oil was produced in 1951. This field has performed water flooding since 1960. Recently, this field has been considered for polymer flooding due to its high permeability, medium viscosity of oil (20 cP), low reservoir temperature (30 °C) and injection of low salinity water resulting in low polymer concentration requirements. In 2009, an integrated study concluded that polymer injection is the most promising recovery method after water flooding at reasonably cost.

Also, high efficiency of polymers in increasing water viscosity for the 8 TH reservoir conditions was confirmed by laboratory experiments. A core flood experiment showed the displacement with polymer injection would lead to an incremental recovery of more than 20% of oil in place after water flooding.

Water Injection Fall-Off Test Interpretation

This well was drilled in March 1980 and located in a lower horizon of the Matzen field. In preparation for the polymer injection, water injection was performed in well Schönkirchen C 1 and fall-off tests were performed. The well was re-completed and an injection test was performed to investigate the reservoir properties: - permeability and skin and also to determine whether water injection occurred under fracturing conditions.

Based on the rate and pressure data from the injection test of the well Schönkirchen C 1 pressure transient analysis is performed. General well and reservoir property data are listed in Table 1.

Table 1: Well and reservoir parameters of Schönkirchen C 1

<i>Parameter</i>	<i>Value</i>
Well type	Vertical
Type of test	Fall-off tests
Well radius, r_w (m.)	0.108 m. (8 1/2" bit size)
Perforated interval (m.)	1,250 – 1,255
Water salinity (ppm)	11,000
Layer Temperature (°C)	30
Formation volume factor	1.008 (from correlation)
Water viscosity, μ_w (cP)	0.803 (from correlation)
Total compressibility, c_t (psi ⁻¹)	6.11×10^{-6} (from correlation)

Figure 2 shows the log-log plot of the two fall-off period. The same stabilization of the two tests confirms the calculated reservoir parameters. Figure 3 and Figure 4 show the matching results of the first and second fall-off test periods. These two tests suggest negative skin as a results of well acidizing and permeability of 550 md.

Table 2 summarizes the matching parameters of the two fall-off tests. An upward trend seen in the 2nd fall-off log-log plot may indicate a reservoir boundary, decreasing in mobility (k/μ) or, an interference of the other producers. The possibility of seeing a drainage area of the other producers is more likely. Therefore, reservoir model is designed for infinite large systems. These matching parameters are then used in reservoir simulation.

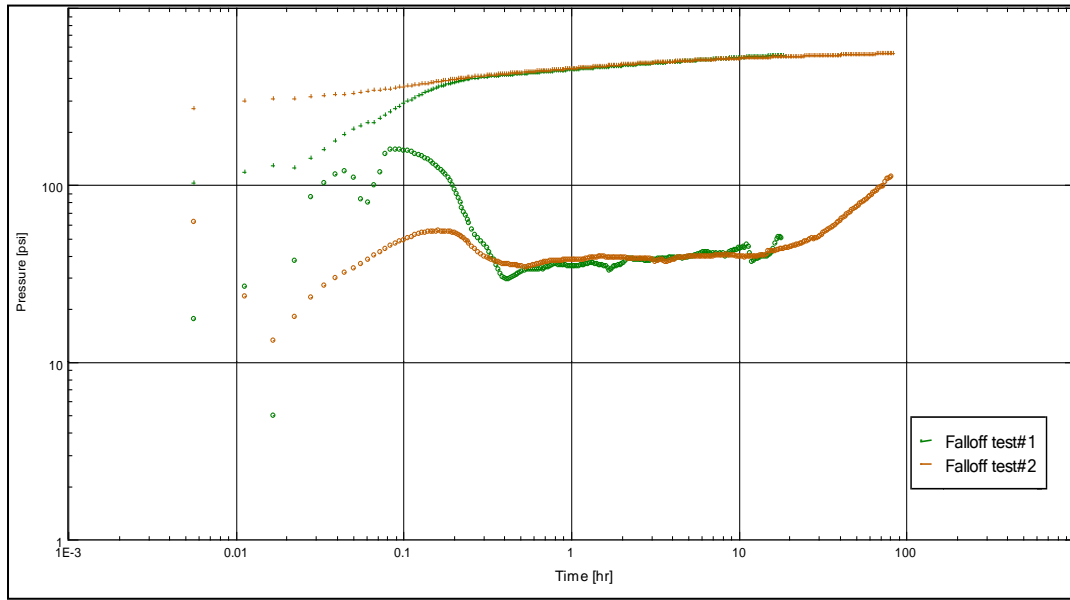


Figure 2: Log-log plot of the two water injection fall-off test of the well Schönkirchen C 1

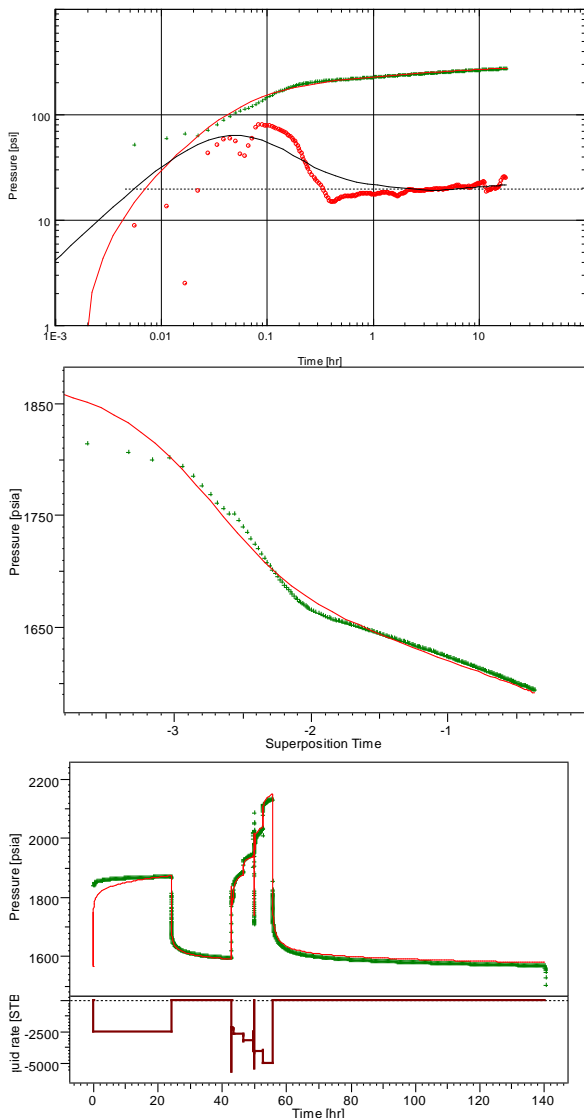


Figure 3 Log-log plot, semi-log plot and history plot of the 1st fall-off test

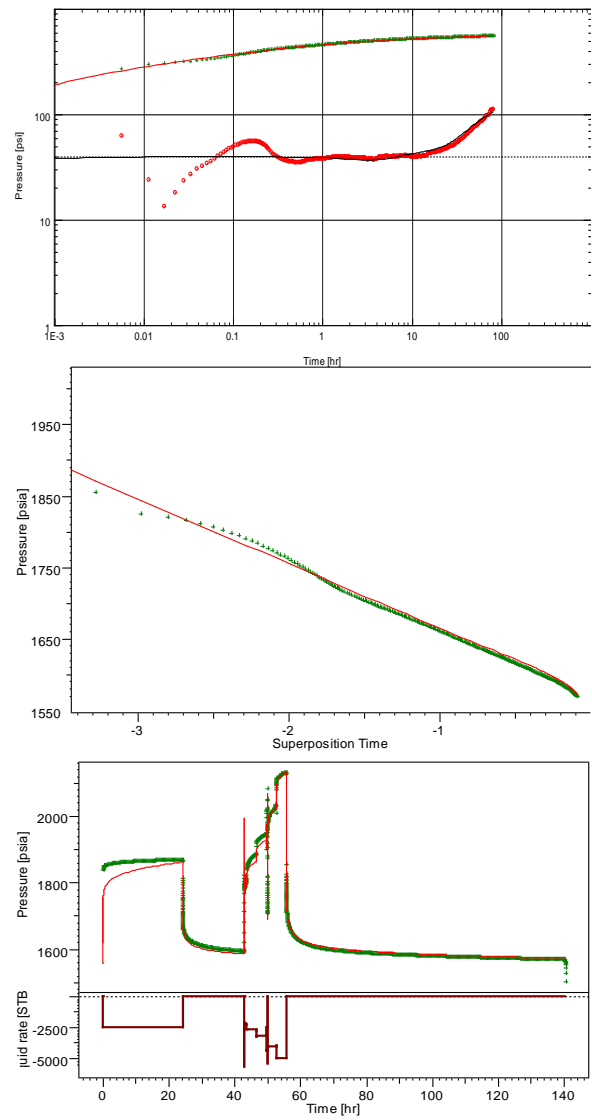


Figure 4: Log-log plot, semi-log plot and history plot of the 2nd fall-off test

Table 2: Matching parameters of the two water injection fall-off tests of the well Schönkirchen C 1

<i>Parameter</i>	<i>Fall-off#1</i>	<i>Fall-off#2</i>
Reservoir	Homogeneous	Homogenous
Boundary	Infinite	Rectangle
Initial pressure, p_i (psia)	1568	1557
Permeability, k (md)	550	550
Skin, S	-1.06	-1.27
Wellbore storage, C (bbl/psi ⁻¹)	0.03	8.69×10^{-6}

Radial Simulation Model Description

The reservoir data derived from the pressure transient analysis were used to construct a radial finite difference model. In this model, it is assumed that close to the injector, negligible amount of oil is present. Hence, the model was initialized as water filled.

The water and the injected non-Newtonian fluid are assumed to form a homogeneous mixture; therefore, single phase exists in the inner zone. Gravity and capillary effects are negligible.

By inferring the reservoir properties from the two water injection fall-off tests, radial grid reservoir models are generated. One-layer systems are used for homogeneous case and five-layer systems are used for heterogeneous case.

The radial grid cell size of 0.1 meter is modeled to locate the exact polymer front position and to reduce numerical dispersion.

First, the reservoir simulations of the history water injection fall-off tests are performed to check the validity of the reservoir parameters obtained from pressure transient analysis.

The simulated pressure gives a good match with the pressure and rate history of the water injection fall-off tests. During history matching, the well and reservoir parameters such as well radius, porosity, thickness, water viscosity, effective permeability and total compressibility are kept constant, except from initial pressure adjusted to 1550 psia to achieve a good history match of the water fall-off test.

Figure 5 shows the history matching of the two fall-off tests with homogeneous and heterogeneous reservoirs. The first water injection fall-off test does not match well because of changing skin between these two tests. However, this gives a confidence to apply the reservoir model with non-Newtonian fluid. The reservoir and fluid properties in reservoir simulation are listed in Table 3 and the apparent polymer viscosity is a function of polymer concentration is provided in Table 4.

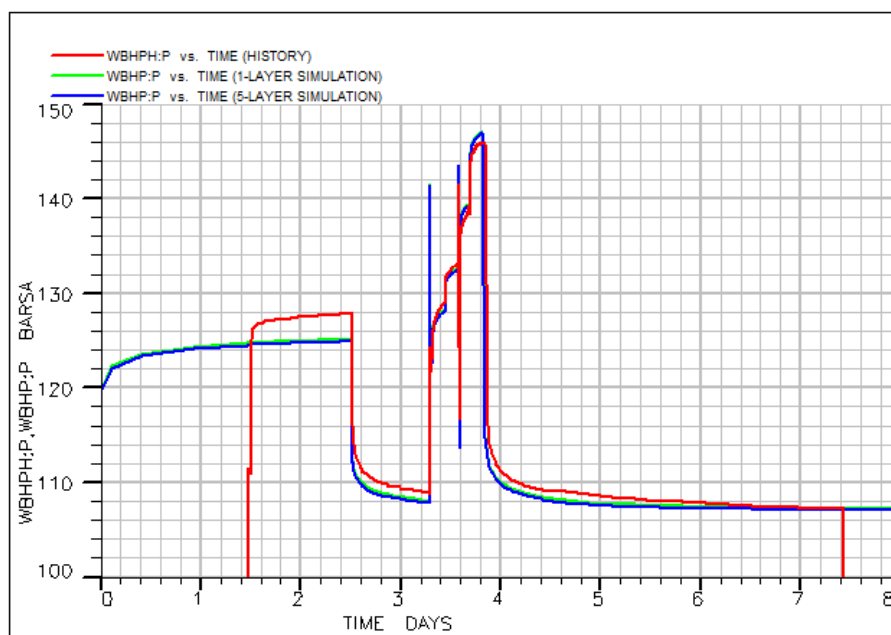


Figure 5: History matching of the water injection fall-off tests for homogeneous and heterogeneous reservoirs

Table 3: Reservoir and fluid properties in reservoir simulation

<i>Parameters</i>	<i>Value</i>
Effective permeability, k_{eff} (md)	550
Initial water saturation, S_{wi}	1.0
Initial pressure, p_i (psia)	1550
Pressure at external radius, p_e (psia)	1550
Well radius, r_w (m)	0.108
Thickness, h (m)	5
Porosity, Φ	0.27
System Compressibility, c_t (psi^{-1})	6.18×10^{-6}
Water viscosity, μ_w (cP)	0.8
External boundary, r_e (m)	1000

Table 4: Polymer Solution Viscosity at Different Polymer Concentration

<i>Polymer concentration, $C(\text{kg}/\text{m}^3)$</i>	<i>Polymer viscosity, $\mu_{\text{app}}(\text{cP})$</i>
0.0	1
0.5	11
1.0	31
1.5	44

Interpretation of polymer solution injection fall-off tests without shear-thinning effect

After validating the radial model with the historical data from the water injection fall-off tests, the model was used to investigate the effect of polymer injection and to determine whether pressure transient analysis could be used to determine in-situ polymer solution viscosity and location of the front. In this paragraph, polymer solutions were injected in the simulation without including Non-Newtonian behavior.

Analysis of Fall-Off Tests after Different Injecting Periods

Figure 6 shows the effect of polymer injection time when the reservoir is filled with water. Water is injected into the one-layer reservoir at a stable rate of $300 \text{ m}^3/\text{d}$ for 1, 6, 23, 51, 90 and 141 days which are equal to the polymer front distance from the well of 10, 20, 40, 60, 80 and 100 m. The external boundary is 1000 m.

The log-log plot of the different injecting time is shown in Figure 7. In some cases, a first straight line cannot be observed, though the simulated data assume no wellbore storage. Also, a second straight line does not develop owing to the dominant boundary effect during the fall-off tests. Therefore, it is practical to do multiple fall-off tests to find the two stabilizations periods. Smooth data and straight lines are a result of computer generated values without including noise.

The log-log pressure plots demonstrate the response for polymer solution system to the outer boundary of water zone. This indicates the scheme to detect the location of the polymer front. Front radius of simulated pressure can be calculated by pressure transient analysis proposed by Bixel 1967, Brown 1985 and Olarewaju 1987. The apparent viscosity can be estimated by using the mobility ratio by assuming water viscosity in the outer zone is known. Table 5 lists all data used for polymer front radius and apparent polymer viscosity calculation. It shows that the calculated polymer front radius coincides with the radius applied volumetric balance equation in the reservoir simulation. Also, the mobility ratio gives a good estimate in apparent polymer viscosity.

Four parameters obtained from the pressure transient analysis are time match, mobility, diffusivity and storativity. They affect the front radius calculation. For example, the determination of front radius is a proportional to square root of time match; hence, if the time match is underestimated by a factor of two, then the front radius is underestimated by the square root of the same factor. Also, it implied that errors are greater because of an error in mobility and diffusivity.

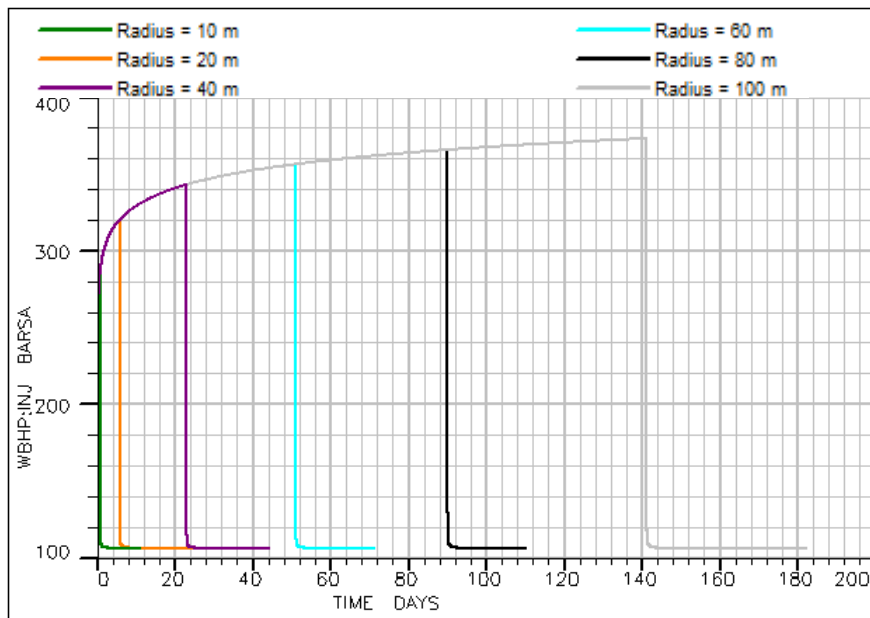


Figure 6: Pressure response as a function of injection period

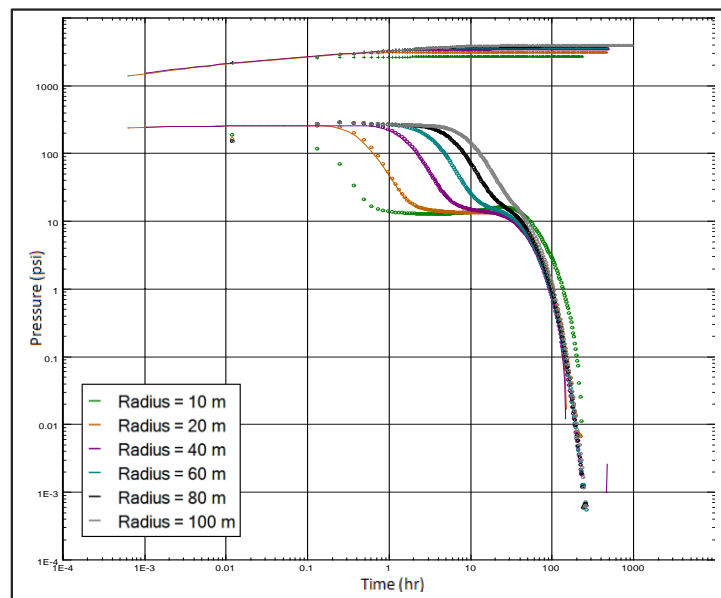


Figure 7: Log-log bottom-hole pressure as a function of injection time

Table 5: Injection time effect of composite system for simulated fall-off tests

Injection time, t_{inj} (days)	1	6	23	51	90	141
Cumulative injection (m^3)	300	1800	6900	15300	27000	42300
Volumetric Metric, R (m)	10	20	40	60	80	100
Initial pressure, p_i (psia)	*	1556	1542	1533	1541	**
k (md)	*	550	550	550	550	**
M	*	0.048	0.048	0.048	0.047	**
D	*	0.047	0.047	0.049	0.050	**
S	*	1.021	1.021	0.980	0.940	**
μ_{app} (cP)	*	16.7	16.7	16.7	17.09	**
μ_{app} error (%)	*	-1.8%	-1.8%	-1.8%	0.5%	**
R (m)	*	22.2	40.8	60.6	81.4	**
R error (%)	*	11.0%	2.0%	1.0%	1.8%	**
r_e (m)	*	980.6	982.2	980.9	970.2	**

* Not enough data point to match the first stabilization.

** Not enough data point to match the second stabilization.

Effect of Heterogeneity

To study the effect of heterogeneity, a layer-system reservoir was modeled. For simplicity, one-layer reservoir is divided to five-layer reservoir which has the same total permeability thickness was introduced. It is assumed that each layer is isolated by the others or zero vertical permeability.

This study investigates four cases. The first reservoir model is one-layer reservoir with 550 md permeability and 5 m constant thickness used as a baseline for studying the effect of 5-layer reservoir models. The second model is five-layer system with constant 550 md permeability with 1 m thickness each. The third model is 1 m thickness each and 330, 440, 550, 660, and 770 md permeability top-down reservoirs. The fourth model looks the same as the third model except that the permeability is changed to 100, 440, 550, 660, 1000 md. All the models, polymer solutions are injected at constant rate of 300 m³/d corresponding to 40 m volumetric front radius from the well. The external boundary is 1000 m.

It can be seen on pressure transient analysis shown in Figure 8 that the heterogeneity indicate external boundary earlier than homogenous system. In other words, pressure transient in the highest permeability sand sends the fastest response to the external boundary though the total kh in a comingled layer are the same. As a result, the fourth model, the highest permeability of 1000 md sees the boundary effect earlier than the other models. Though its prediction of polymer viscosity and polymer front is reasonable, the external radius has an almost 30% error. Furthermore, the number of reservoir layer has less effect on pressure transient analysis if the permeability is the same. It can be seen that the constant five layer of 550 md shows the same response as one layer reservoir model. Table 6 shows the analyzed data.

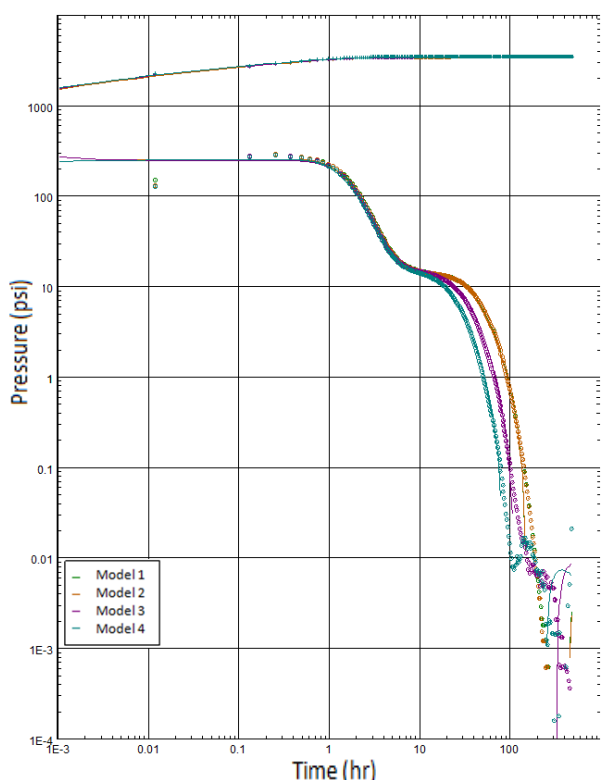


Figure 8: Log-log bottom-hole pressure for one-layer and five-layer reservoirs

Table 6: Heterogeneity effect of composite system for simulated fall-off tests

Model	1	2	3	4
k-Layer 1 (md)	-	550	330	100
k-Layer 2 (md)	-	550	440	440
k-Layer 3 (md)	-	550	550	550
k-Layer 4 (md)	-	550	660	660
k-Layer 5 (md)	-	550	770	1000
k _{eff} (md)	550	550	550	550
t _{inj} (day)	23	23	23	23
p _i (psia)	1542	1542	1539	1539
M	0.048	0.048	0.048	0.048
D	0.047	0.047	0.050	0.047
S	1.021	1.021	0.96	1.021
μ _{app} (cP)	16.7	16.7	16.7	16.7
μ _{app} error (%)	-1.8%	-1.8%	-1.8%	-1.8%
R (m)	40.8	40.8	40.2	39.6
R error (%)	2.0%	2.0%	0.5%	-1.0%
r _e (m)	982.2	982.2	825.6	725.1
r _e error (%)	-1.8%	-1.8%	-17.4%	-27.5%

Effect of Polymer Concentration

The effect of polymer concentration on transient pressure behavior was investigated for injection of polymers into a water reservoir with a constant pressure boundary of 1000 m. This is done by maintaining a stable 300 m³/d injection rate for 23 days with 0.25, 0.75, and 1.25 kg/m³ of polymer concentration. The pressure response was calculated for a single-layer reservoir model.

As seen in Figure 9, the flowing bottom-hole pressure increases with time and polymer concentration. The log-log plot for the three different polymer concentrations is shown in Figure 10. Unlike the case of Newtonian fluid, a significant increase in the pressure response indicates a change in transmissibility (kh/μ) and a behavior of composite reservoir system. It shows that the

polymer front radius and apparent polymer viscosity determined by applying pressure transient analysis does not depend on polymer concentration as shown in Table 7 which summarizes all the analyzed data. The radial composite scheme can predict well for apparent viscosity and polymer front radius.

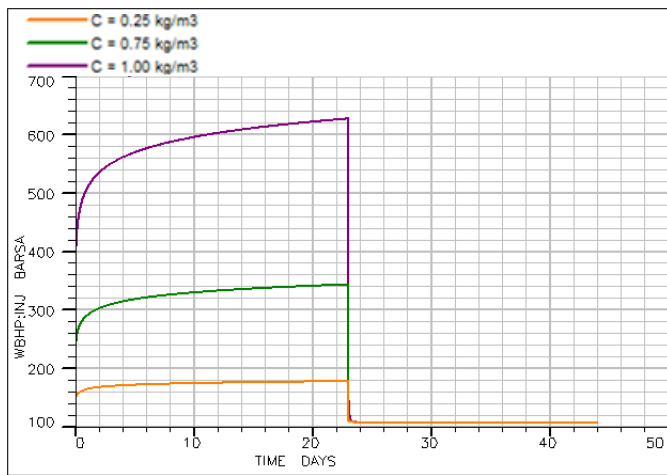


Figure 9: Pressure response as a function of polymer concentration

Table 7: Effect of polymer concentration

Polymer Concentration (kg/m ³)	0.25	0.75	1.25
t _{inj} (days)	23	23	23
μ _{app} (cP)	5	17	38
p _i (psia)	1543	1542	1545
M	0.160	0.048	0.022
D	0.170	0.047	0.021
S	0.941	1.021	1.048
R (m)	42.5	40.8	40.6
r _e (m)	985	982	973
R error (%)	5.9%	2.0%	1.5%
μ _{app} (cP)	5	16.7	36.5
μ _{app} error (%)	0.0%	-1.8%	-3.95%

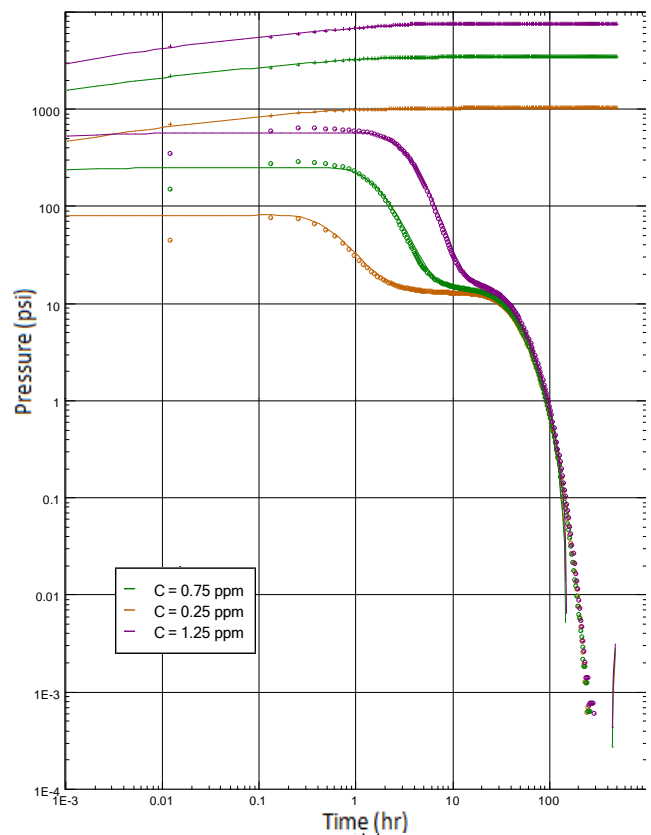


Figure 10: Log-log plot of simulated bottom-hole pressure fall-off test as a function of polymer concentration

Effect of Permeability Reduction

The study performed by W. Gogarty (1967) showed a permeability reduction in a core test during polymer flooding. The permeability reduction results from the effect of small pore blocked by flowing large polymer molecules. As a result, polymer flooding efficiency reduces as decreasing in permeability. In reservoir simulation, this effect is treated through the term of residual resistance factor (RRF), an indication of the permanence of the permeability reduction effect. It expresses as the mobility of brine solution before and after contact with polymer.

The effect of permeability reduction is studied by injecting the polymer fluid for 23 days with RRF of 1, 1.5 and 2 in the reservoir with external boundary of 2000 m. 1 RRF means no decreases in mobility of a polymer solution in comparison with the flow of brine or water. It shows in Figure 11 that the injection pressure increases as RRF increases due to the nature of mobility-reducing interaction between polymer solution and a porous media system. This effect causes injectivity problems that induce an increasing in injection pressure or a decreasing in polymer injection rate.

In practice, the permeability reduction (RRF) can be determined in the laboratory and permeability can be calculated. As seen in the analyzed data Table 8, the apparent viscosity and polymer front is calculated by pressure transient analysis in case polymer solution is interacted with the a porous media. Polymer front radius determination and mobility ratio resulting in viscosity value closely match the reservoir simulation input. Generally, mobility ratio and diffusivity ratio for permeability reduction case is determined by dividing both values of no interaction case with residual resistance factor.

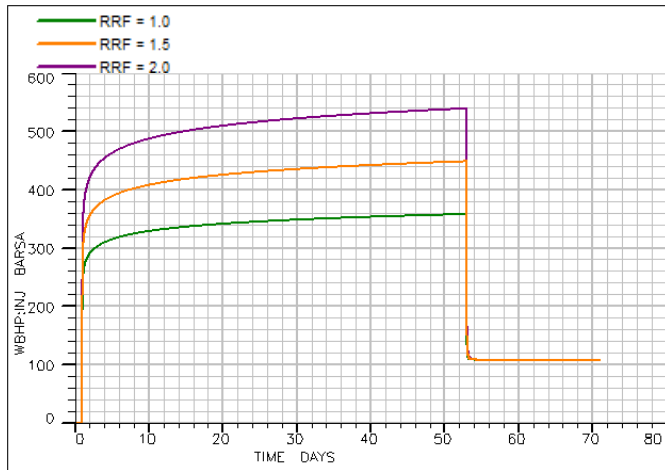


Figure 11: Effect of permeability reduction

Table 8: Permeability reduction effect of composite system for simulated fall-off tests

RRF	1.0	1.5	2.0
t_{inj} (days)	23	23	23
μ_{app} (cP)	17	17	17
p_i (psia)	1544	1539	1543
M	0.047	0.032	0.024
D	0.048	0.032	0.025
S	0.979	1.00	0.960
R (m)	41.2	38.7	38.4
R error (%)	3.0%	-3.25%	-4.0%
r_e (m)	2001	1909	1930
k (md)	550	367	275
μ_{app} (cP)	17	16.7	16.7
μ_{app} error (%)	0.0%	-1.8%	-1.8%

Interpretation of polymer solution injection fall-off tests with shear-thinning effect

Theoretically, polymer behaves as a non-Newtonian fluid which apparent viscosity depends on the shear rate. The relationship between apparent viscosity and shear rate is shown in Figure 12. It shows that in the laboratory, the measured viscosity of this polymer solution follows the power law model.

The parameters K and n in power law correlation can be determined by plotting the shear rate and viscosity on the logarithmic scales. The slope and intercept are an indicative of exponent n and K. It appears n is equal to 0.71 and K is equal to 32.25 cP.s^{0.29}. This indicates the polymer solution is shear-thinning fluid.

Then, this shear rate is converted to Darcy velocity and polymer viscosity as shown in Figure 13. Three relationships are parallel because they are applied the same power law parameters K and n with different polymer concentration. This process is used to be able to simulate shear-thinning behavior, since the reservoir simulation program used (ECLIPSE 100) requires polymer viscosity versus flow velocity as input data.

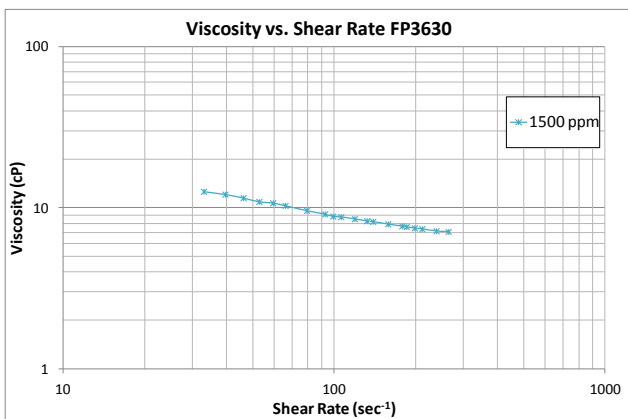


Figure 12: Lab measurement of polymer solution of FP 3630

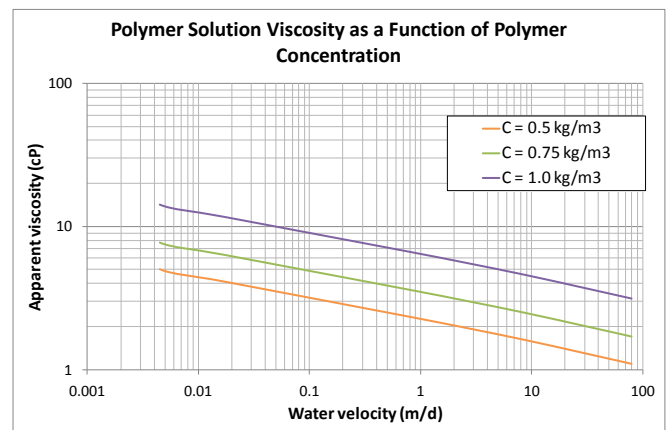


Figure 13: the Correlation between Polymer Solution Viscosity and Darcy velocity Used in Reservoir Simulation

Polymer solutions with a concentration of 0.5, 0.75 and 1.0 kg/m³ were injected. The injection rate is constant at 300 m³/d for 51 days corresponding to the volumetric polymer front radius of 60 m. The external boundary of 2000 m is selected to clearly observe the second radial flow stabilization.

Figure 14 shows the polymer viscosity in the reservoir with shear-thinning fluids. Near the wellbore region fluid flows with high velocity; therefore, viscosity is low due to shear-thinning behavior and the apparent viscosity is then increasing due to low velocity experienced deep in the reservoir. At the front radius, the viscosity should equal the water viscosity at 0.8 cP; however, because of the numerical dispersion no sharp front contact can be seen. Figure 15 shows the comparison between polymer with and without shear-thinning behavior at 0.75 kg/m³ polymer concentration. Flowing bottom-hole pressure for shear-thinning behavior is less than that for without shear-thinning behavior because of its less viscosity as a result of shear-thinning effect.

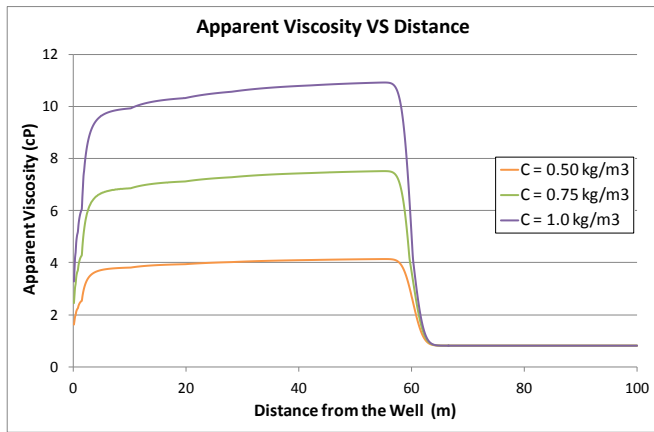


Figure 14: Apparent viscosity as a function of well distance and polymer concentration

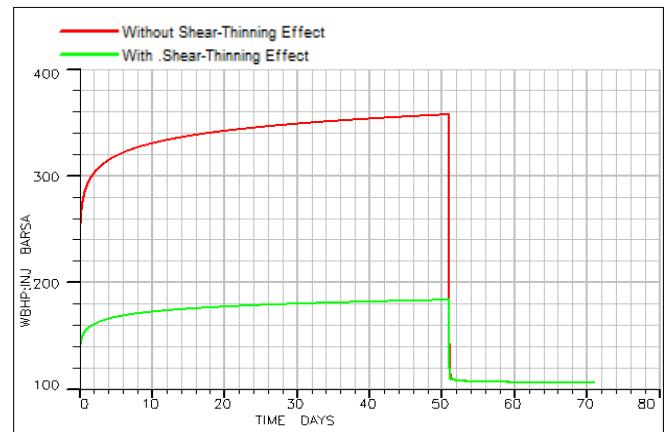


Figure 15: Bottom-hole reservoir pressure with and without shear-thinning effect at 0.75 kg/m³ polymer concentration

The flowing bottom-hole pressure response was also studied as a function of the polymer concentration. Figure 16 shows the reservoir pressure as a function of polymer concentration with shear-thinning behavior. Similar to the case without shear-thinning effect, the pressure response increases as polymer concentration increases.

As polymer-containing fluid propagates to the reservoir, fall-off tests were simulated. The simulated pressure responses were then interpreted using a pressure transient analysis program. Figure 17 compares the log-log plot with different polymer concentration. Unlike the Newtonian fluids in previous section, the second stabilization is not smooth owing to changing mobility. However, pressure transient analysis gives the polymer front and external boundary closed to the input in reservoir simulation at 60 m and 2000 m respectively. However, if the mobility ratio is high or less contrast in viscosity between inner and outer zone, the location of the polymer front cannot be determined precisely using pressure transient analysis.

The apparent polymer viscosity in the reservoir simulation is calculated by averaging the values in the reservoir grid from the well to the polymer front. This viscosity is then compared to the calculated viscosity from mobility ratio in well test analysis.

The analyzed data is summarized in the Table 9. The results show that mobility ratio obtained from pressure transient analysis gives the apparent polymer viscosity prior to well shut-in or during injection period. One might expect that in fall-off period, the viscosity should increase owing to the decrease in velocity. However, as observed in the reservoir simulation the viscosity distribution remains equal to that at the instant of shut-in as shown in Figure 18. This is analogue to what happens in lean gas-condensate reservoir below the saturation pressure (Novosad 1996), (Wheaton 2000) and (Jones 1987).

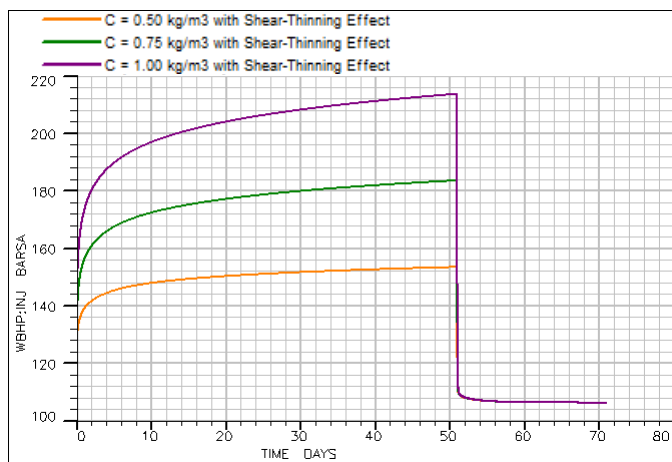


Figure 16: Pressure response with shear thinning effect as a function of polymer concentration

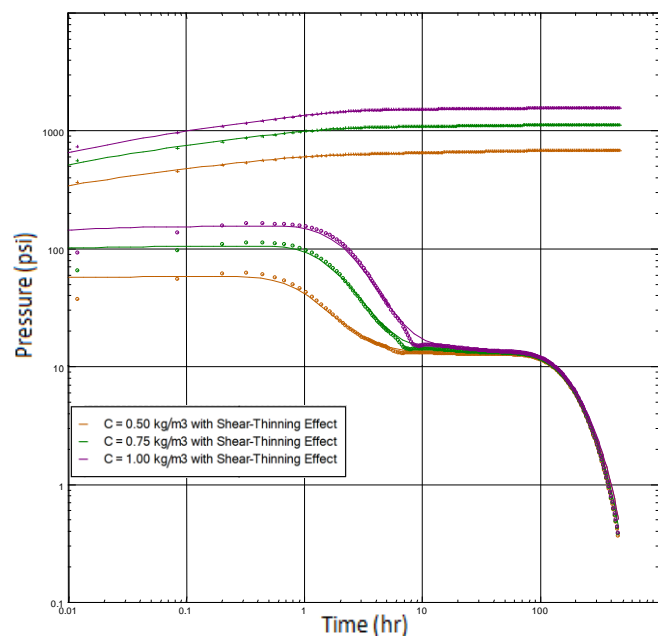
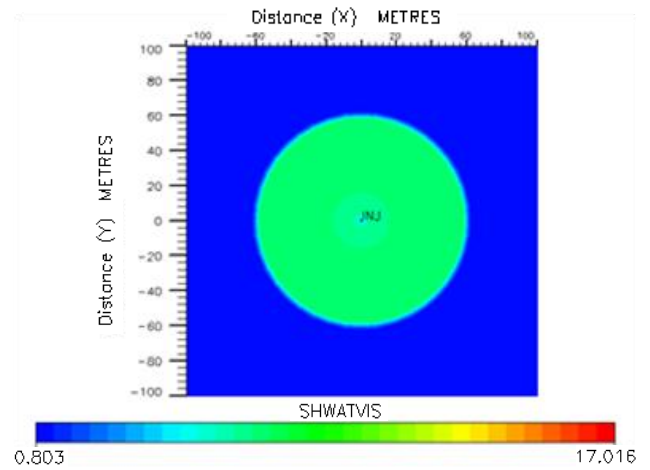


Figure 17: Log-log plot of simulated bottom-hole pressure fall-off test with Shear thinning fluids as a function of polymer concentration

Table 9: Effect of polymer concentration in shear-thinning behavior

Polymer Concentration (kg/m^3)	0.50	0.75	1.00
t_{inj} (days)	51	51	51
μ_{app} (cP)	3.71	6.62	9.55
p_i (psia)	1542	1543	1547
M	0.209	0.115	0.081
D	0.226	0.118	0.079
S	0.925	0.975	1.025
μ_{app} calculated (cP)	3.84	6.98	9.91
μ_{app} error (%)	3.6%	5.4%	3.6%
R (m)	66.5	64.5	61.6
R error (%)	10.8%	7.5%	2.7%
r_e (m)	1947	1950	1980
r_e error (%)	-2.7%	-2.5%	-1.0%

**Figure 18: Polymer viscosity with shear thinning behavior at instant shut-in for 0.75 kg/m^3 polymer concentration**

Summary and Conclusions

The objective of this study was to determine the apparent polymer viscosity and polymer front radius by applying pressure transient analysis techniques to the flow of Newtonian and non-Newtonian fluids in porous media. The non-Newtonian fluids of interest are pseudoplastic (shear-thinning). The applicability of polymer injection fall-off tests was investigated.

First, it is important to perform water injection fall-off tests before performing polymer injection fall-off tests. A baseline of water injection fall-off test gives information about reservoir permeability and near wellbore damage. These two parameters are used to reduce the uncertainty in pressure transient analysis in polymer injection tests.

Second, without shear-thinning fluid both polymer front radius and the mobility ratio are determined by pressure transient analysis techniques and then the apparent polymer viscosity can be calculated. Also, when a second semi-log straight line develops, its straight line length decreases with the increasing flowing time, polymer concentration and heterogeneity.

Third, it is practical to conduct multiple polymer injection fall-off tests for observing two clear stabilizations because the interpretation of pressure transient analysis has influenced by the duration of the injection time and the external boundary. For example, relatively small volume of polymer injection the first stabilization cannot develop, but massive volume the second stabilization cannot be observed. Also, in case of heterogeneous reservoir, pressure transient analysis finds the external boundary earlier than expected because the highest permeability zone sends the fastest response to the boundary.

Forth, in shear-thinning fluid pressure transient analysis gives a good estimate of the polymer fluid front; however, the errors increase if the difference in viscosity is small. Moreover, the mobility ratio predicts the apparent polymer viscosity during the polymer injection period rather than that during fall-off period.

Nomenclature

p_i	= initial reservoir pressure, psia
p_{wD}	= dimensionless wellbore pressure drop
Δp_{wD}	= wellbore pressure drop, psi
S_{wi}	= initial water saturation
r_w	= well radius, m
h	= thickness, m
R	= polymer front radius, m
r_e	= external boundary, m
μ_{app}	= apparent polymer viscosity, cP
μ_w	= water viscosity, cP
k_{eff}	= effective permeability, md
Φ_i	= inner zone porosity
Φ_o	= outer zone porosity
q_{inj}	= injection rate, m^3/d
t_{inj}	= injection time, d
B	= formation volume factor

V_s	= sweep volume, m^3
c_t	= total compressibility, psi^{-1}
C	= wellbore storage, bbf/psi^{-1}
R_D	= dimensionless discontinuity radius
t_{DX}	= dimensionless intersection time
t_x	= intersection time, hr
t_e	= deviation time, hr
t_{De}	= dimensionless deviation time
M	= mobility ratio
D	= diffusivity ratio
S	= storativity ratio
K	= consistency index, $cP.s^{n-1}$
n	= power law exponent
γ	= Shear rate, s^{-1}
u	= superficial flow rate, m/s

Acknowledgements

First of all, I would like to express my deepest and sincere gratitude to my project advisors, Professor Alain Gringarten and Torsten Clemens, for their continuous supervision throughout this study. They always spent their time in giving me advice and teaching me how to express my ideas to the study. Their valuable guidance was very useful in completing this study. Besides my advisors, I would like to express my gratefulness to Mr. Markus Zechner. Without his corporation I could not have gotten such relevant data.

Lastly I would like to thank my family: my parents and my brothers. I could not have accomplished this project without a great support and encouragement to pursue my interests. Also I would like to thank all Lecturers and Department Staffs for good administrations, and all friends in supporting me.

References

- Bixel, H.C., and van Poollen, H.K. "Pressure Drawdown and Buildup in the Presence of Radial Discontinuities." *SOC. Pet. Eng. J.*, 1967: 301-309.
- Brown, L.P. "Pressure Transient Behavior of the Composite Reservoir." *SPE 14316*, 1985.
- Chang, H.L., Zhang, Z.Q., Wang, Q.M., Xu Z.S., and Guo Z.D. SPE, Daqing Oilfield Co. Ltd., PetroChina, H.Q., and Cao, X.L. Shengli Oilfield Co. Ltd., Sinopec Sun., and Q. , Xinjiang Oilfield Co. Ltd., PetroChina and Qiao. "Advances in Polymer Flooding and Alkaline/Surfactant/Polymer Processes as Developed and Applied in the People's Republic of China." *SPE 89175*, 2006: 84-89.
- Christopher, R. H. and Middleman, S. "Power-Law Flow through a Packed Tube." *Ind. and Eng. Chem. Fund.*, 1965: 422.
- Clark, S. R., Pitts, M.J., and Smith, S.M. "Design and Application of an Alkaline-Surfactant-Polymer Recovery System to the West Kiehl Field." *SPE 17538*, 1993: 172-179.
- Da Prat, G., Bockh, A., and Prado, L. "Use of Pressure Falloff Tests to Locate the Burning Front in the Miga Field, Eastern Venezuela." *SPE 13667*, 1985.
- Dauben, D. L. and Menzie, D. E. "Flow of Polymer Solutions through Porous Media." *J. Pet. Tech.*, 1967: 1065-1073.
- Du, Y., and Guan, L. "Field-Scale Polymer Flooding: Lessons Learned and Experiences Gained During Past 40 Years." *SPE 91787*, 2004.
- Eggenschwiler, M., and Ramey, H.J., Jr., and Satman, A. "Interpretation of Injection Well Pressure Transient Data in Thermal Oil Recovery." *SPE 8908*, 1980.
- Gogarty, W. B. "Mobility Control with Polymer Solutions." *SPE*, 1967: 161-173.
- Gogarty, W.B. "Rheological Properties of Pseudoplastic Fluids in Porous Media." *Soc. Pet.Eng.*, 1967: 149-160.
- Han, M., Xiang, W., Zhang, j., Jiang, W., and Sun, F. "Application of EOR Technology by Means of Polymer Flooding in Bohai Oil Fields." *SPE 104432*, 2006.
- Horne, R. N., Satman, A., and Grant, M.A. "Pressure Transient Analysis of Geothermal Wells with Phase Boundaries." *SPE 9274*, 1980.
- J.R. Gilman, S.B. Hinchman, and M.A. Svaldi., "Using Polymer Injectivity Tests To Estimate Fracture Porosity." *SPE 25880*, 1993.
- Jones, J. R., Vo, D. T., and Raghavan R. "Performance Predictions for Gas Condensate Reservoirs." *SPE 16984*, 1987.
- MacAllister, D. J. "Pressure Transient Analysis of CO₂ and Enriched-Gas Injection and Production Wells." *SPE 16225*, 1987.
- Marshall, R. J. and Metzner, A. B. "Flow of Viscoelastic Fluids through Porous Media." *Ind. and eng. Chem. Fund.*, 1967: 393.
- McKinley, R.M., Jahns, H.O., and Harris, W.W. "Non-Newtonian Flow in Porous Media." *AICHE*, 1966: 17-20.
- Merill, L.S., Jr., Kazemi, H. and Gogarty W.B. "Pressure Falloff Analysis in Reservoir with Fluid." *J.Pet.Tech.*, 1974: 809-818.
- Messner, G. L. and Williams, R. L. "Application of Pressure Transient Analysis in Steam Injection Wells." *SPE 102781*, 1982a.
- Messner, G. L. and Williams, R. L. "Further Investigation of Pressure Transient Testing in Steamflood Projects." *SPE 11087*, 1982b.
- Muskat, M. *The Flow of Homogeneous Fluids through Porous Media*. New York: McGraw-Hill Book Co., Inc., 1937.
- Novosad, Z. "Composition and Phase Changes in Testing and Producing Retrograde Gas Wells." *SPE 35645*, 1996.
- Odeh. "Flow Test Analysis for a Well with Radial Discontinuity." *J. Pet. Tech.*, 1969: 207-210.
- Olarewaju, J. S., Lee. W. J. and Lancaster, D. E. "Type- and Decline-Curve Analysis with Composite Models." *SPE 17055*, 1987: 21-23.
- Onyekonwu, M. O., Ramey, H. J. Jr., and Brigham, W. E. "Application of Superposition and Pseudosteady state Concepts to Thermal

- Recovery Well Tests." *SPE 15536*, 1986.
- Onyekonwu, M. O., Ramey, H. J., Jr., Brigham, W. E. and Jenkins, R. "Interpretation of Simulated Falloff Tests." *SPE 12746*, 1984.
- Pye, D. J. "Improved Secondary Recoery by Control of Water Mobility." *J. Pet. Tech.*, 1964: 911-916.
- Ramey, H.J., Jr. "Approximate Solutions for Unsteady Liquid Flow in Composite Reservoirs." *J. Can. Pet. Tech.*, 1970: 32-37.
- Sadowski, T.J. "Non-Newtonian Flow Through Porous Media,II Experimental." *Trans.,Soc.Rheol*, 1965: 251-271.
- Smith, F.W. "The behavior of Partially Hydrolyzed Polyacrylamide Solution in Porous Media." *J. Pet. Tech.*, 1970: 148-156.
- Szabo, M. T.,. "Laboratory Investigations of Factors Influencing Polymer Flood Performance." *Trans. AIME 259*, 1975: 338-346.
- Teeuw, D., and Hesselink, F. T. "Power-Law and Hydrodynamic Behavior of Biopolymer Solutions in Porous media." *SPE8982*, 1980: 28-30.
- Van Pollen, H. K. "Transient Tests Find Fire Front in an In-situ Combustion Project." *Oil and Gas Journal* , 1965: 78-80.
- Van Poolen, H. K. "Radius of Drainage and Stabilization Time Equations." *Oil and Gas Journal*, 1964: 138-146.
- Walsh Jr., John W., Ramey Jr. H.J, Brigham, W.E. "Thermal Injection Well Falloff Testing." *SPE 10227*, 1981.
- Wang, F.H.L., Duda, J.L. and Klaus, E.E. "Influences of Polymer Solution Properties on Flow in Porous Media." *SPE 8418*, 1979: 23-26.
- Wattenbarger, R.A. and Ramey, H.J., Jr. "An Investigation of Wellbore Storage and Skin Effects in Unsteady Liquid Flow: 11. Finite Difference Treatment." *SOC. Per. Eng. J.*, 1970: 291-297.
- Wheaton, R. J., Zhang, H. R. "Condensate Banking Dynamics in gas Condensate Fields." *SPE 62930*, 2000.

Appendix A: Milestones in interpretation of polymer solution injection fall-off test study

SPE Paper n°	Year	Title	Authors	Contribution
2157	1969	“Flow Test Analysis for a Well with Radial Discontinuity”	Odeh, A. S.	Find the relationship of the mobility of the two zones and the radial distance to the discontinuity.
PETSOC 70-01-04	1970	“Approximate Solutions For Unsteady Liquid Flow In Composite Reservoirs”	Ramey, H. J.	Generate the approximation solutions to the usual constant-rate radial flow problem for either no-flow or constant-pressure outer boundary conditions and to determine the distance to a discontinuity from flow test data.
8908	1980	“Interpretation of Injection Well Pressure Transient Data in Thermal Oil Recovery”	Eggenschwiler, M., and Ramey, H.J., Jr., and Satman, A..	Propose the concept of pseudosteady-state or material balance calculation to find the radius of swept zone
8982	1980	“Power-Law and Hydrodynamic Behaviour of Biopolymer Solutions in Porous media”	Teeuw, D. and Hesselink, T. F.	Present the equation to adapt Darcy’s law by taking the flow of power-law fluids into accounts
17055	1987	“Type- and Decline-Curve Analysis with Composite Models”	Olarewaju, J. S. and Lee. W. J.	Present the use of pressure and pressure-derivative type curves to improve flow-regime detection and reservoir property estimation with composite models.

Appendix B: Critical Literature Review

SPE 2157

Flow Test Analysis for a Well with Radial Discontinuity

Authors: Odeh, A. S.

Contribution to the understanding of Interpretation of polymer solution injection fall-off tests:

This paper reported correlations to allow the determination of the mobility of the two zones and the radial distance to the discontinuity.

Objective of the paper:

Provide a numerical solution for the interpretation of flow tests which the pressure behavior of well producing from a region bounded by a circular discontinuity.

Methodology used:

Simulate 30 drawdowns and 30 buildups of a unit capacity ratio, of varied mobility ratios, and of varied the radial distance to the discontinuity. Then, examine the results and obtain the correlations in flow test interpretation.

Conclusion reached:

Normal buildup and drawdown plots resulted in an early (first) straight line, a long transition zone and a late (second) straight line.

PETSOC 70-01-04

Approximate Solutions For Unsteady Liquid Flow In Composite Reservoirs

Authors: Ramey, H. J.

Contribution to the understanding of Interpretation of polymer solution injection fall-off tests:

This paper generated the approximation solutions to the usual constant-rate radial flow problem for either no-flow or constant-pressure outer boundary conditions and to determine the distance to a discontinuity from flow test data.

Objective of the paper:

Provide a class of approximate solutions for unsteady flow in composite reservoirs.

Methodology used:

Derive mathematical equations

Conclusion reached:

The particular class of approximate solutions for radial flow problems involving concentric discontinuities appears to offer more than an aid to physical understanding.

SPE 8908

Interpretation of Injection Well Pressure Transient Data in Thermal Oil Recovery

Authors: Eggenschwiler, M., and Ramey, H.J., Jr., and Satman, A.

Contribution to the understanding of Interpretation of polymer solution injection fall-off tests:

Use the concept of pseudosteady-state or material balance calculation to find the radius of swept zone.

Objective of the paper:

Find the distance from injection well to the front for in-situ combustion project.

Methodology used:

Apply numerical Laplace inverter to generate dimensionless bottom-hole pressure as functions of dimensionless time.

Conclusion reached:

The pore volume of swept zone can be more accurately determined by Cartesian graph between pressure vs time.

Comments:

Use material balance equation to find the polymer front from reservoir simulation

SPE 8982

Power-Law and Hydrodynamic Behavior of Biopolymer Solutions in Porous media

Authors: Teeuw, D. and Hesselink, T. F.

Contribution to the understanding of Interpretation of polymer solution injection fall-off tests:

This paper suggests the equation to adapt Darcy's law by taking the flow of power-law fluids into accounts.

Objective of the paper:

Compare the flow equation for power-law fluids with the flow experiments in Bentheim sandstone rock.

Methodology used:

Derive mathematical equations and do core-flow experiments.

Conclusion reached:

1. Derive an equation for laminar flow of shear-thinning fluids in a porous medium by adapting Darcy's law to power-law flow, using Kozeny's model of parallel-bundled capillaries
2. Compare the apparent viscosity between core flow and Kozeny's model by considering the effect of pore-size distribution, continuously fluctuating flow rate, and hydrodynamic chromatography.

Comments:

Improve an equation for laminar flow of shear-thinning fluids to match the core flow experiments.

SPE 17055

Type- and Decline-Curve Analysis with Composite Models

Authors: Olarewaju, J. S. and Lee. W. J.

Contribution to the understanding of Interpretation of polymer solution injection fall-off tests:

This paper presents the use of pressure and pressure-derivative type curves to improve flow-regime detection and reservoir property estimation with composite models.

Objective of the paper:

Present a series of type curve generated from the composite reservoir model.

Methodology used:

Derive partial differential equation and convert in Laplace transformation with the Stehfest algorithm.

Conclusion reached:

State a new technique for pressure transient analysis with composite system parameters.

Comments:

This method is applicable to bounded or infinite-acting reservoirs.

Appendix C: ECLIPSE Reservoir Modeling

ECLIPSE is commercial software for black oil reservoir modeling (ECLIPSE Simulation Software Manuals 2010.1). Two phase options polymer and water are solved as two component system in this study.

3-dimensional radial geometry grids

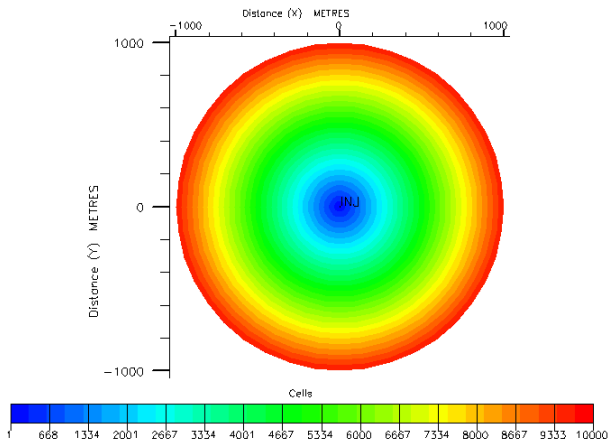


Figure C- 1: Radial grid geometry for 1 km external boundary

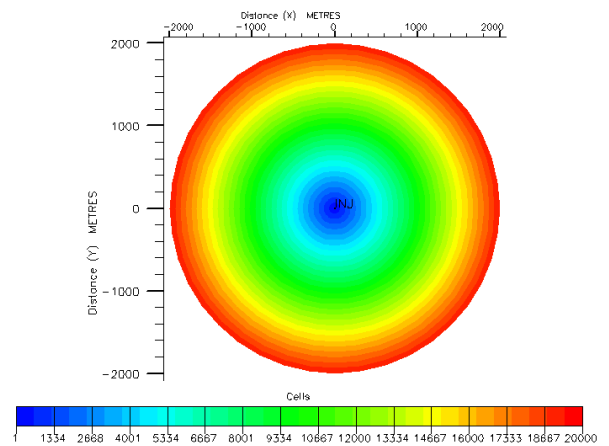


Figure C- 2: Radial grid geometry for 2 km external boundary

Polymer viscosity at $C = 0.25 \text{ kg/m}^3$ without shear thinning behavior

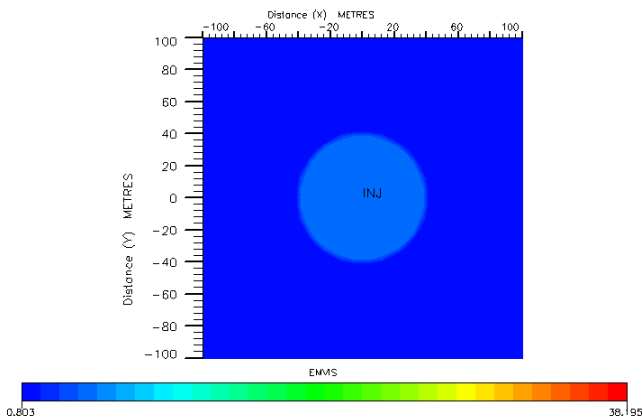


Figure C- 3: Polymer viscosity at $C = 0.25 \text{ kg/m}^3$ without shear thinning at instant shut in

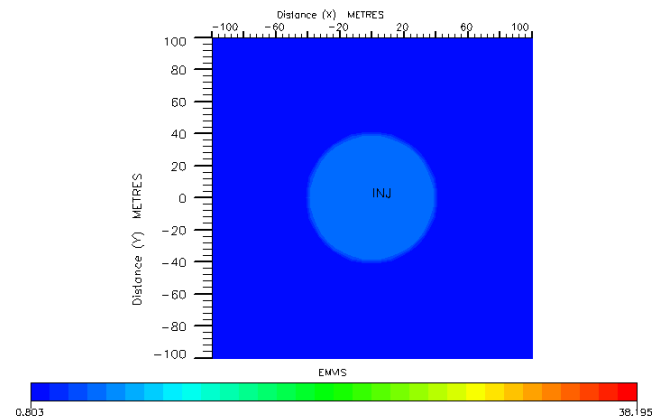


Figure C- 4: Polymer viscosity at $C = 0.25 \text{ kg/m}^3$ without shear thinning behavior for ten days after shut in

Polymer viscosity at $C = 0.75 \text{ kg/m}^3$ without shear thinning behavior

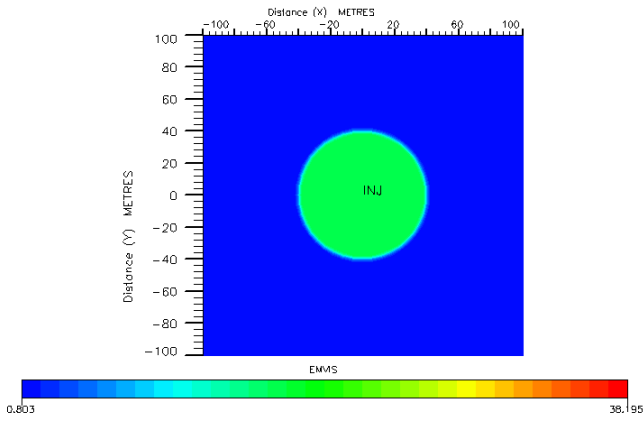


Figure C- 5: Polymer viscosity at $C = 0.75 \text{ kg/m}^3$ without shear thinning at instant shut in

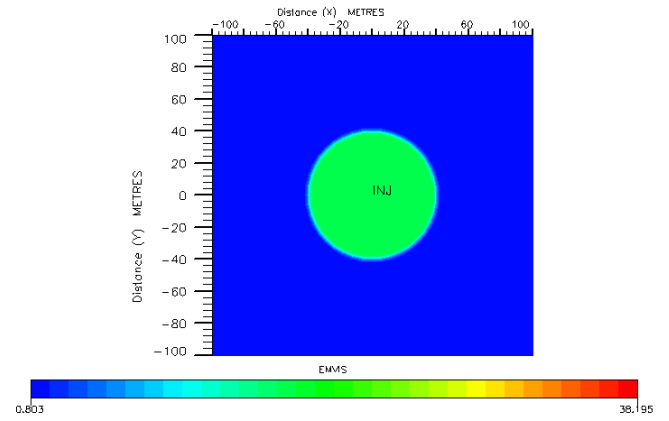


Figure C- 6: Polymer viscosity at $C = 0.75 \text{ kg/m}^3$ without shear thinning behavior for ten days after shut in

Polymer viscosity at $C = 1.25 \text{ kg/m}^3$ without shear thinning behavior

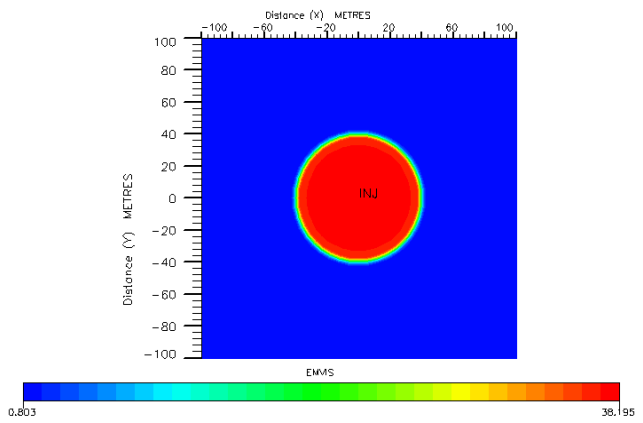


Figure C- 7: Polymer viscosity at $C = 1.25 \text{ kg/m}^3$ without shear thinning at instant shut in

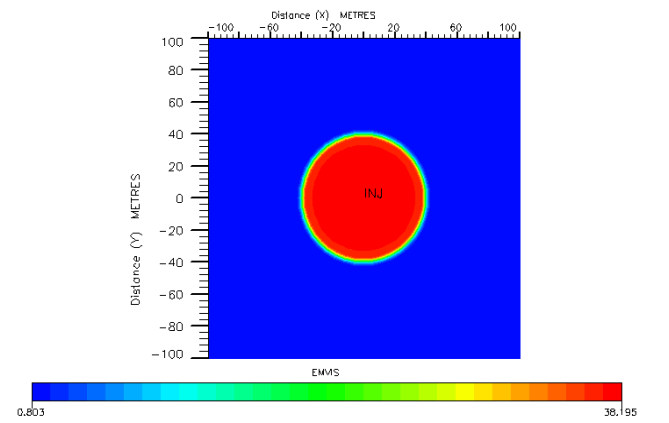


Figure C- 8: Polymer viscosity at $C = 1.25 \text{ kg/m}^3$ without shear thinning behavior for ten days after shut in

Polymer viscosity at $C = 0.75 \text{ kg/m}^3$ with shear thinning behavior

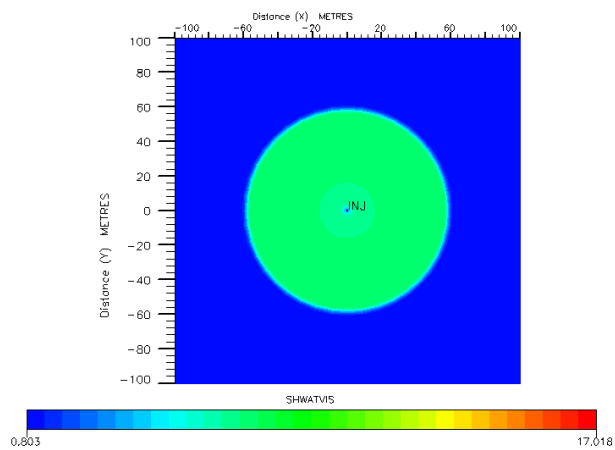


Figure C- 9: Polymer viscosity at $C = 0.75 \text{ kg/m}^3$ with shear thinning behavior for two days before shut in

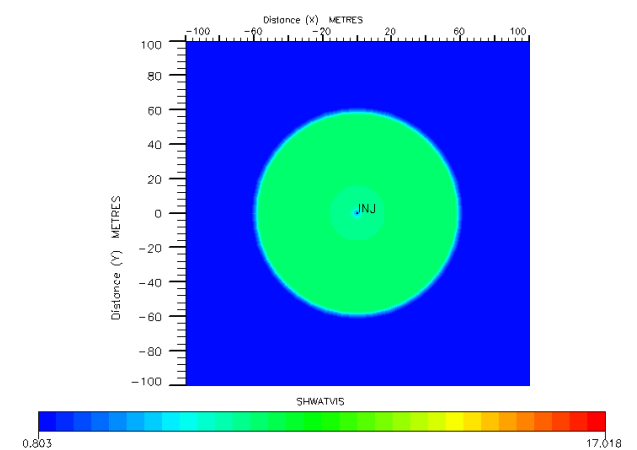


Figure C- 10: Polymer viscosity at $C = 0.75 \text{ kg/m}^3$ with shear thinning behavior for one day before shut in

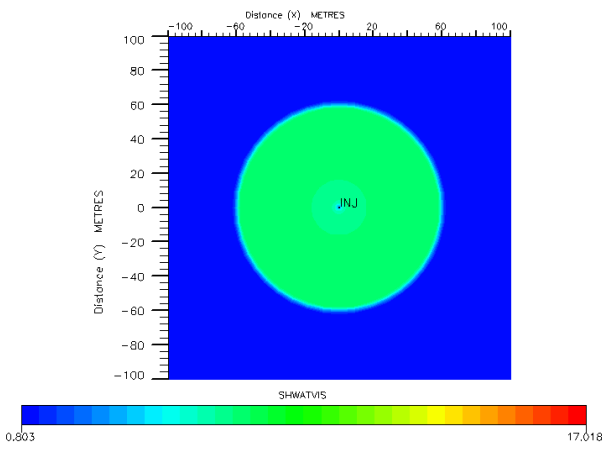


Figure C- 11: Polymer viscosity at $C = 0.75 \text{ kg/m}^3$ with shear thinning behavior at instant shut-in

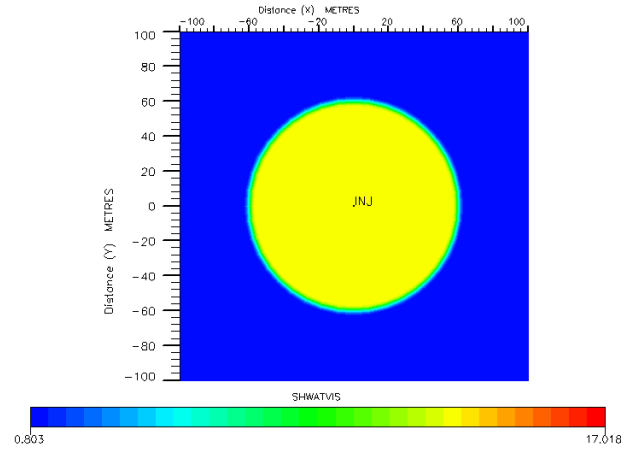


Figure C- 12: Polymer viscosity at $C = 0.75 \text{ kg/m}^3$ with shear thinning behavior for one day after shut in

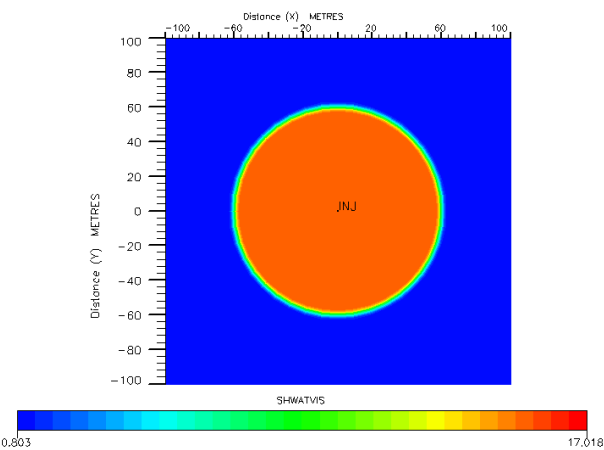


Figure C- 13: Polymer viscosity at $C = 0.75 \text{ kg/m}^3$ with shear thinning behavior for two days after shut in

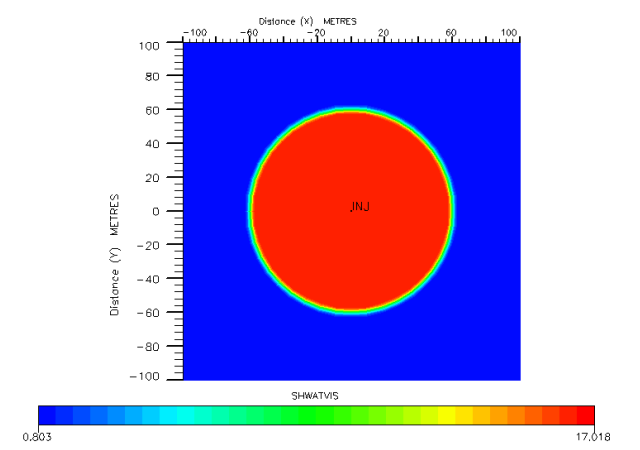


Figure C- 14: Polymer viscosity at $C = 0.75 \text{ kg/m}^3$ with shear thinning behavior for ten days after shut in

Appendix D: Sapphire program

Sapphire is a commercial software for pressure transient analysis (Dynamic Flow Analysis – v4.10.01 - © KAPPA 1988 -2009).

The log-log, semi-log, and simulated history plots are provided. All the models used are homogeneous, vertical and radial composite model with no wellbore storage and skin.

Effect of injection time

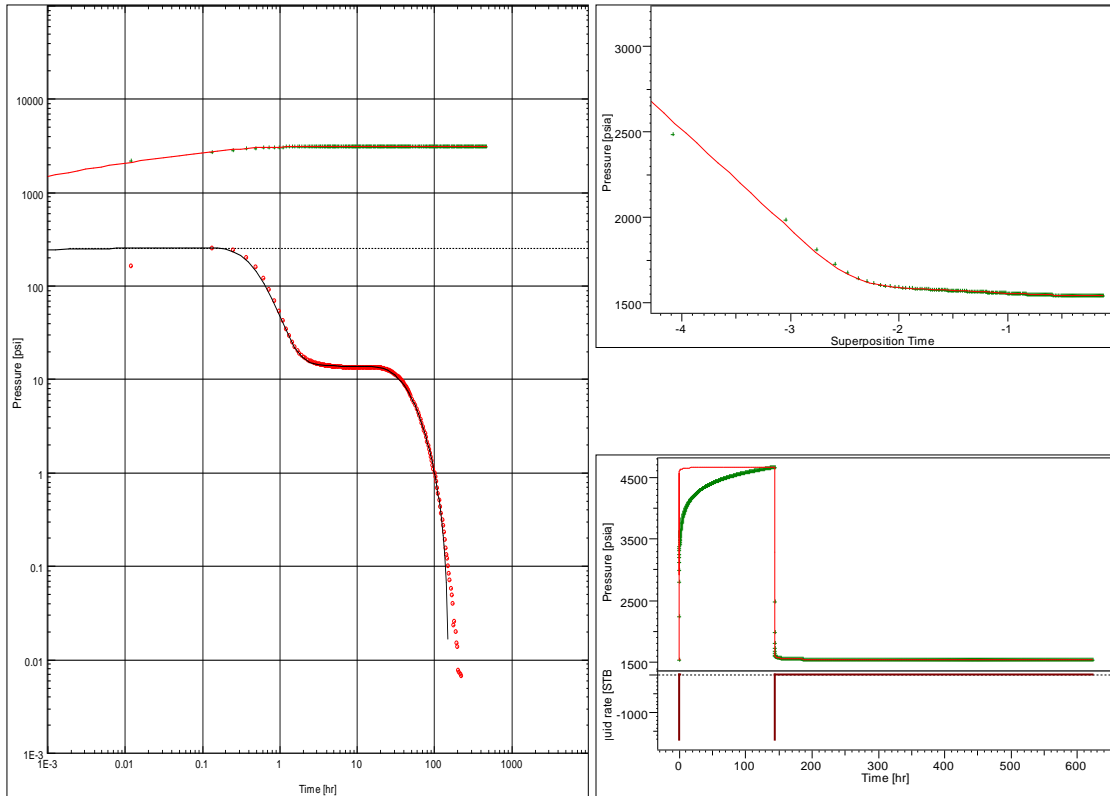


Figure D- 1: Log-log, semi-log and history plot for 6 days polymer injection and R = 20 m

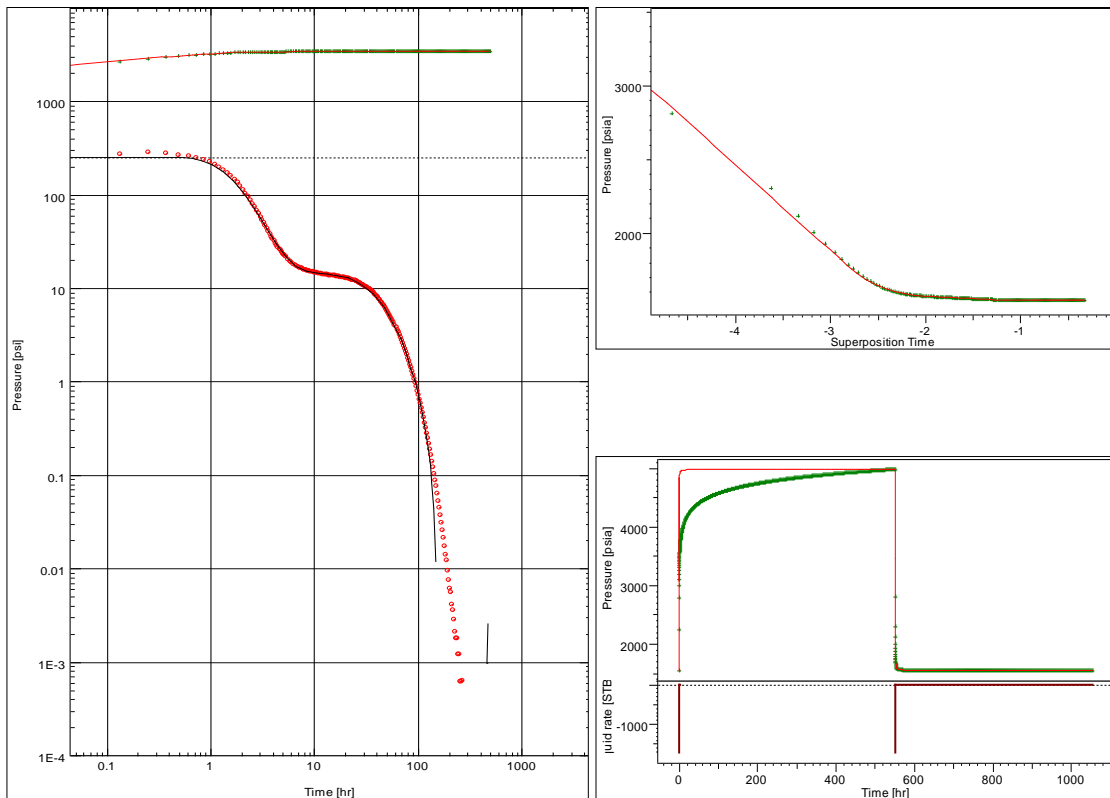


Figure D- 2: Log-log, semi-log and history plot for 23 days polymer injection and R = 40 m

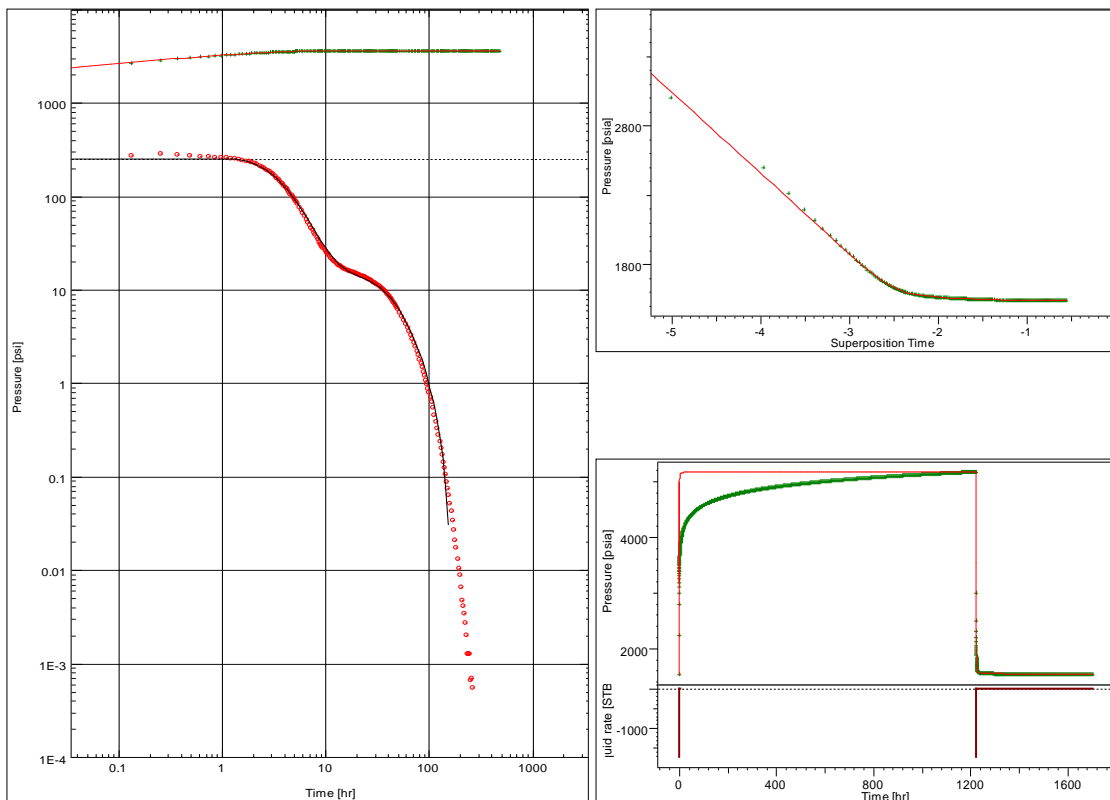


Figure D- 3: Log-log, semi-log and history plot for 51 days polymer injection and R = 60 m

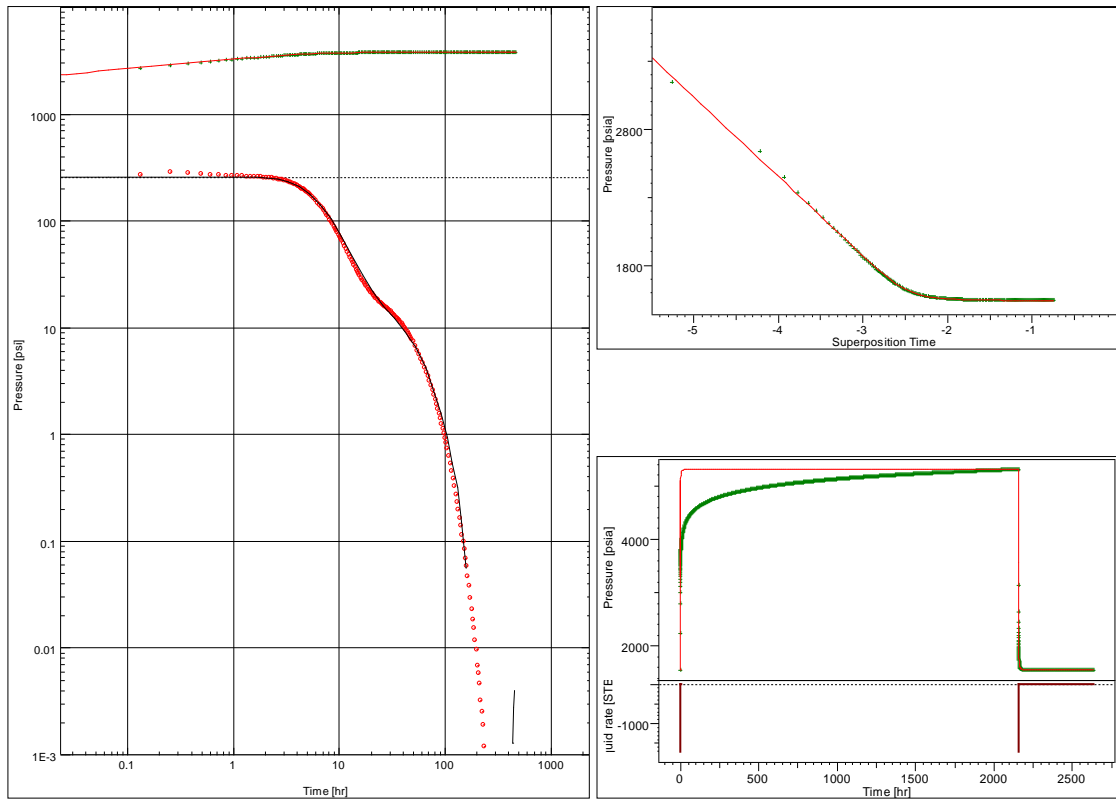


Figure D- 4: Log-log, semi-log and history plot for 90 days polymer injection and R = 80 m

Effect of heterogeneity

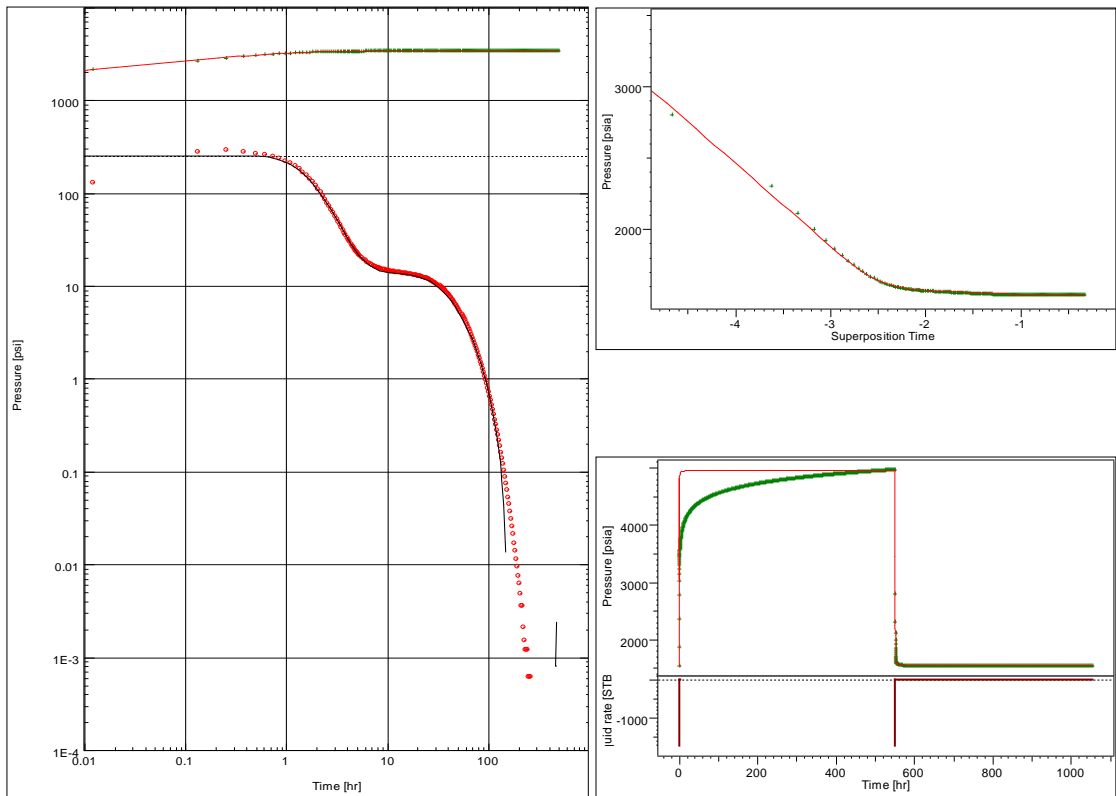


Figure D- 5: Log-log, semi-log and history plot for 23 days polymer injection in the five layers of constant 550 md permeability

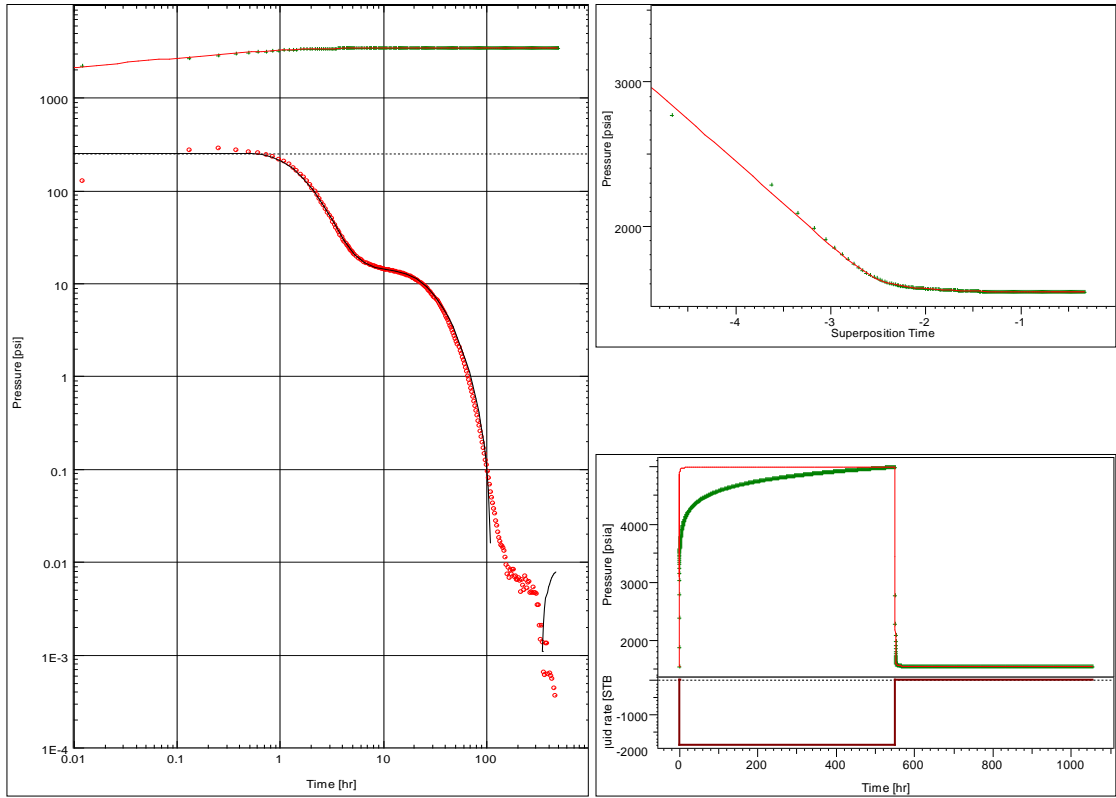


Figure D- 6: Log-log, semi-log and history plot for 23 days polymer injection in the five layers of 330, 440, 550, 660 and 770 md permeability

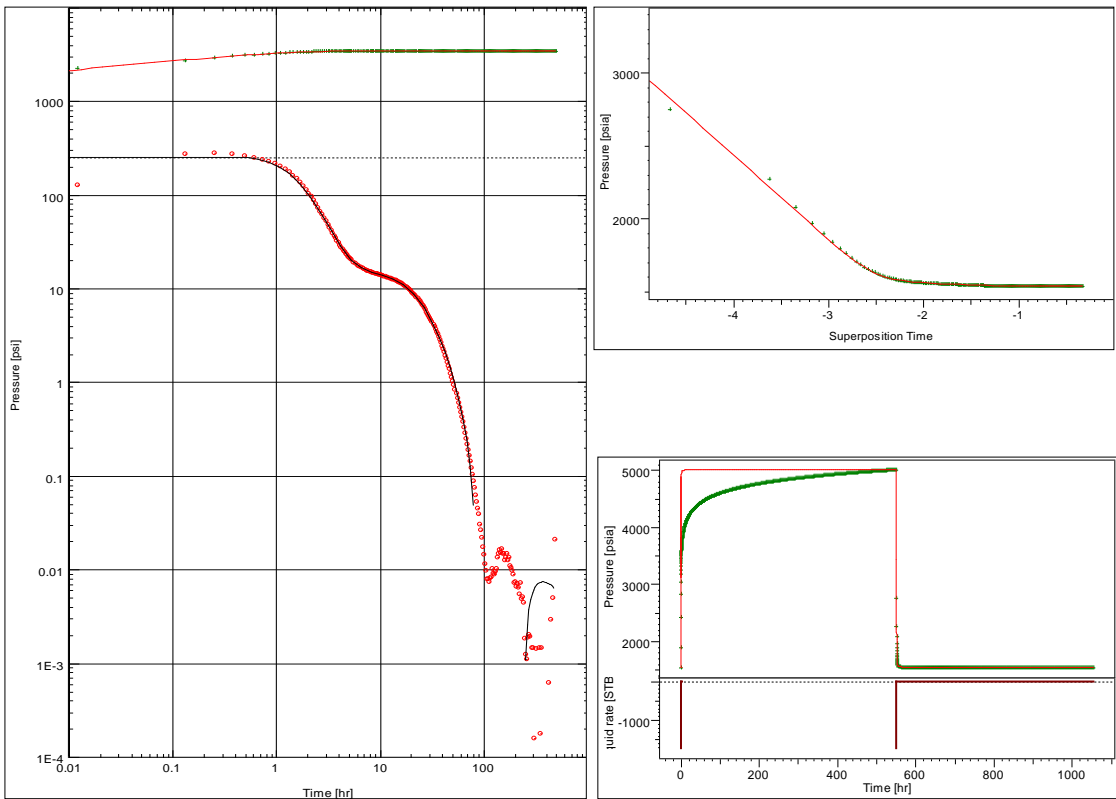


Figure D- 7: Log-log, semi-log and history plot for 23 days polymer injection in the five layers of 100, 400, 550, 600 and 1000 md permeability

Effect of permeability reduction

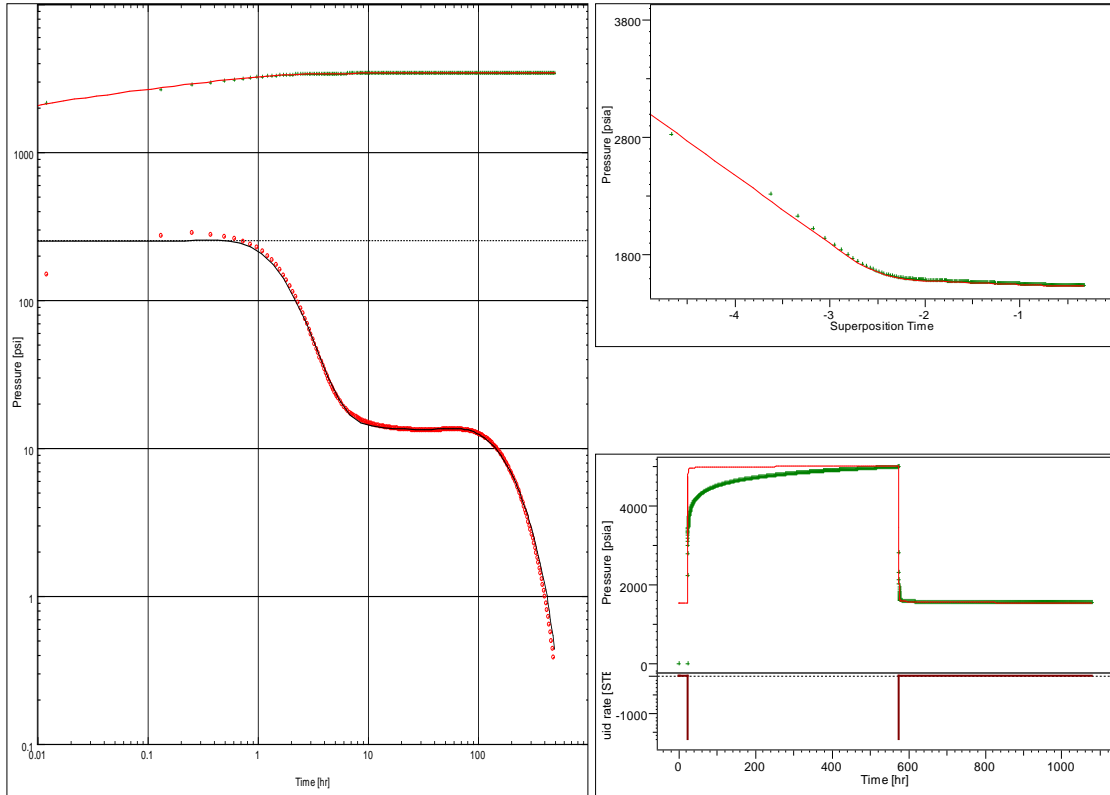


Figure D- 8: Log-log, semi-log and history plot for 23 days polymer injection for RRF = 1.0

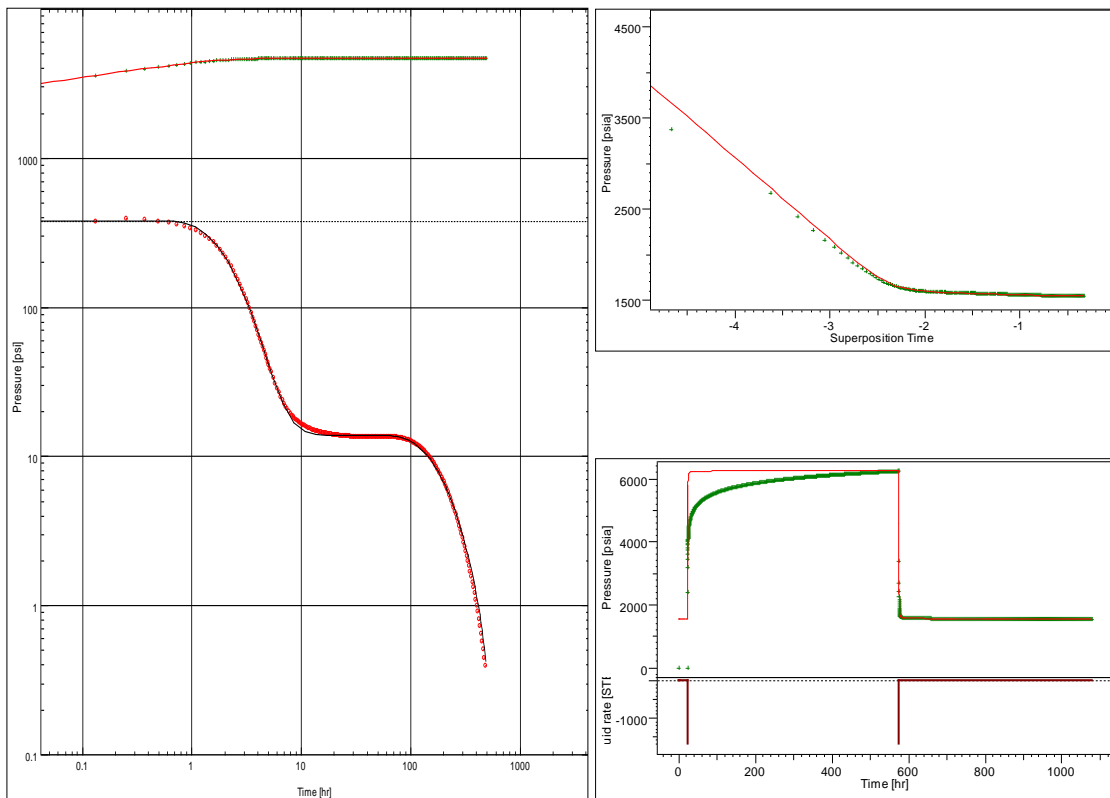


Figure D- 9: Log-log, semi-log and history plot for 23 days polymer injection for RRF = 1.5

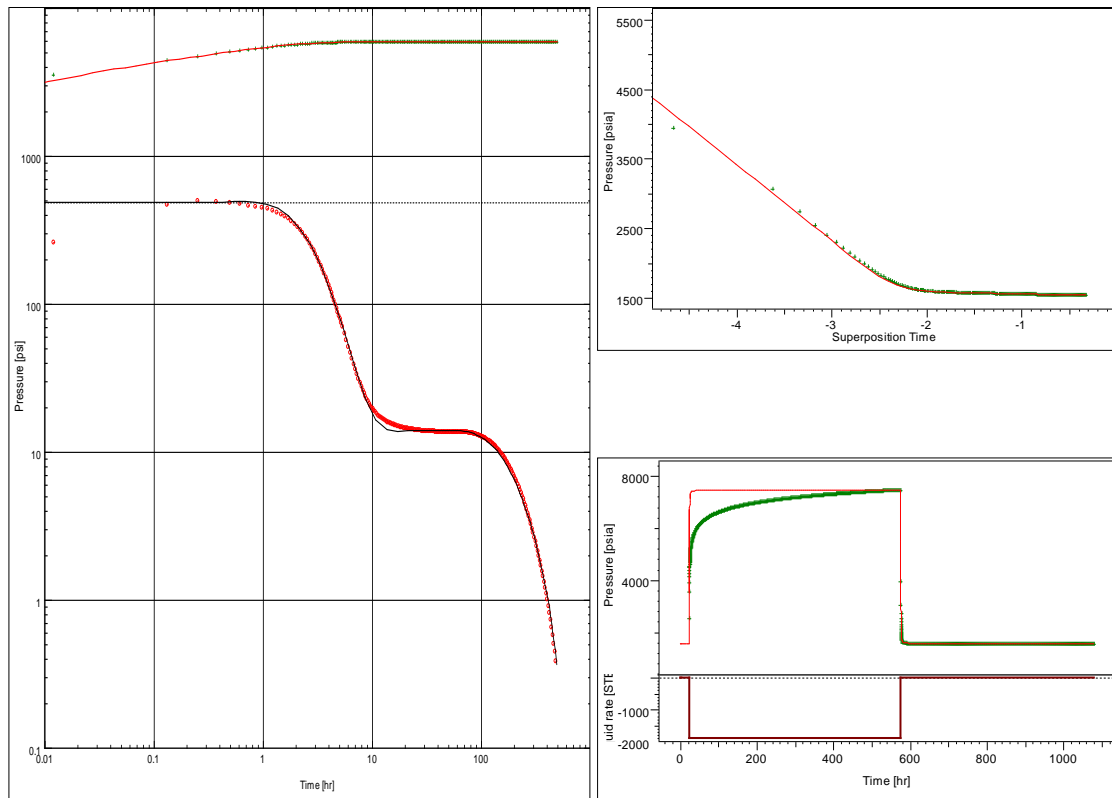


Figure D- 10: Log-log, semi-log and history plot for 23 days polymer injection for RRF = 2.0

Effect of polymer concentration

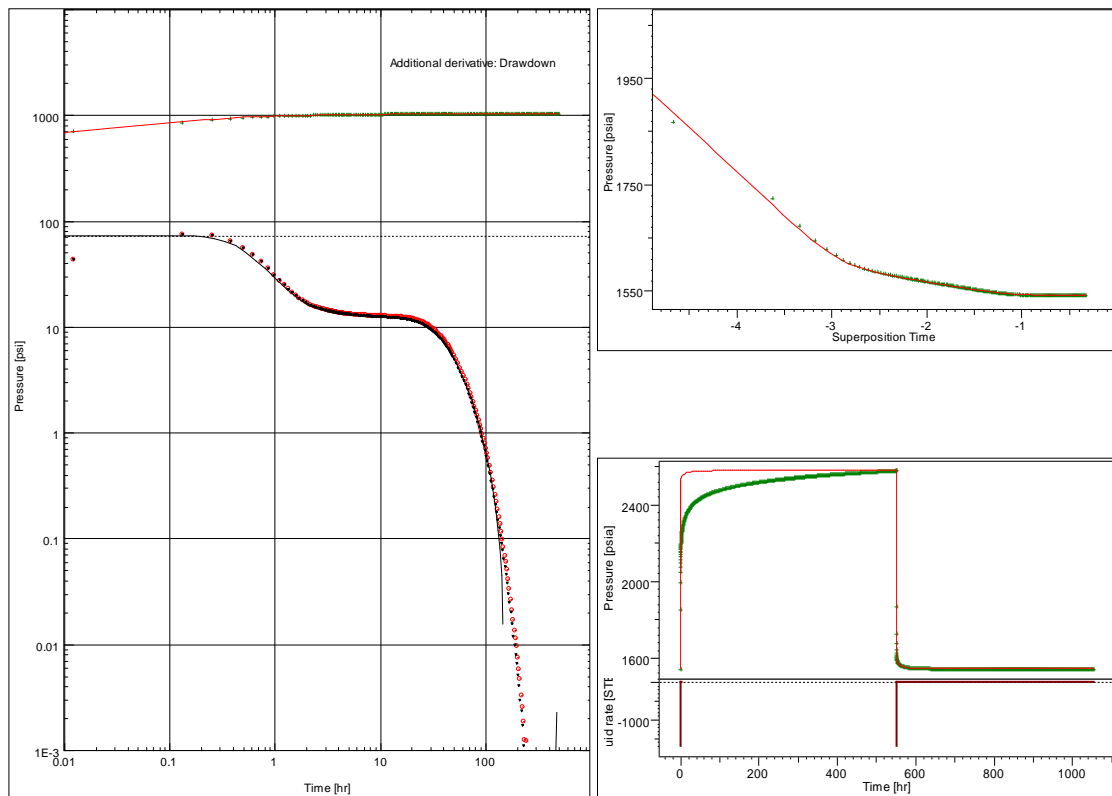


Figure D- 11: Log-log, semi-log and history plot for 51 days polymer injection with $C = 0.25 \text{ kg/m}^3$

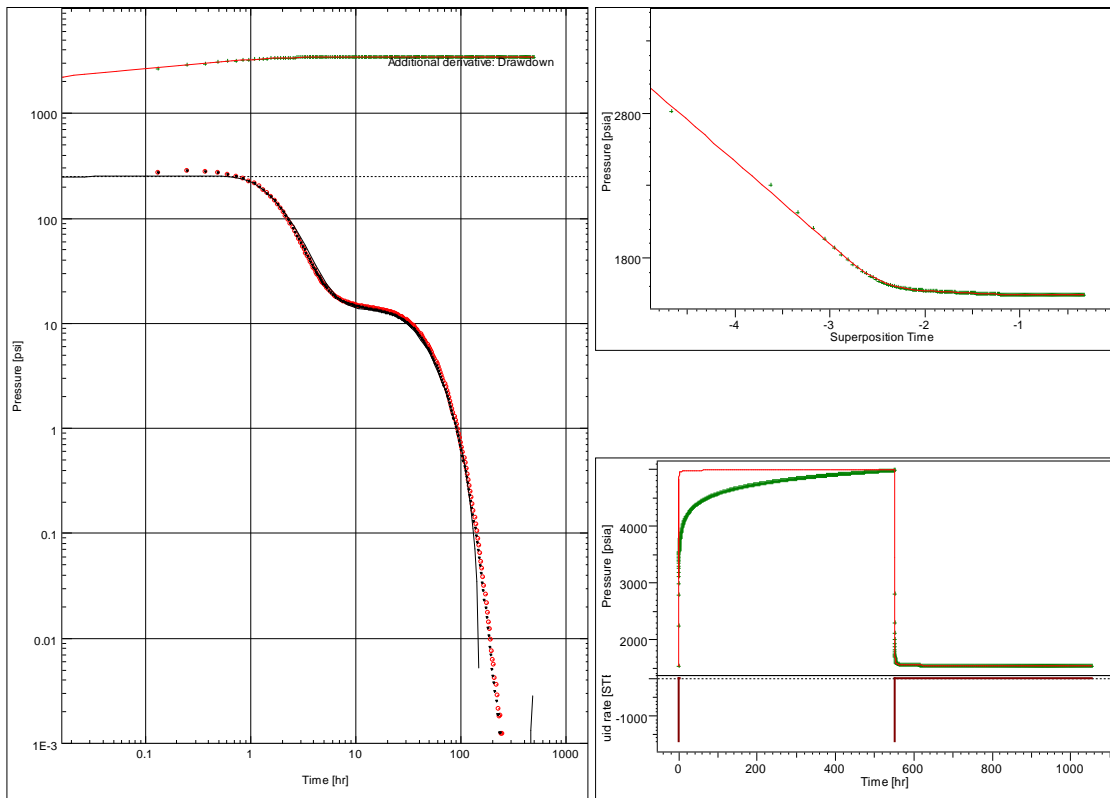


Figure D- 12: Log-log, semi-log and history plot for 51 days polymer injection with $C = 0.75 \text{ kg/m}^3$

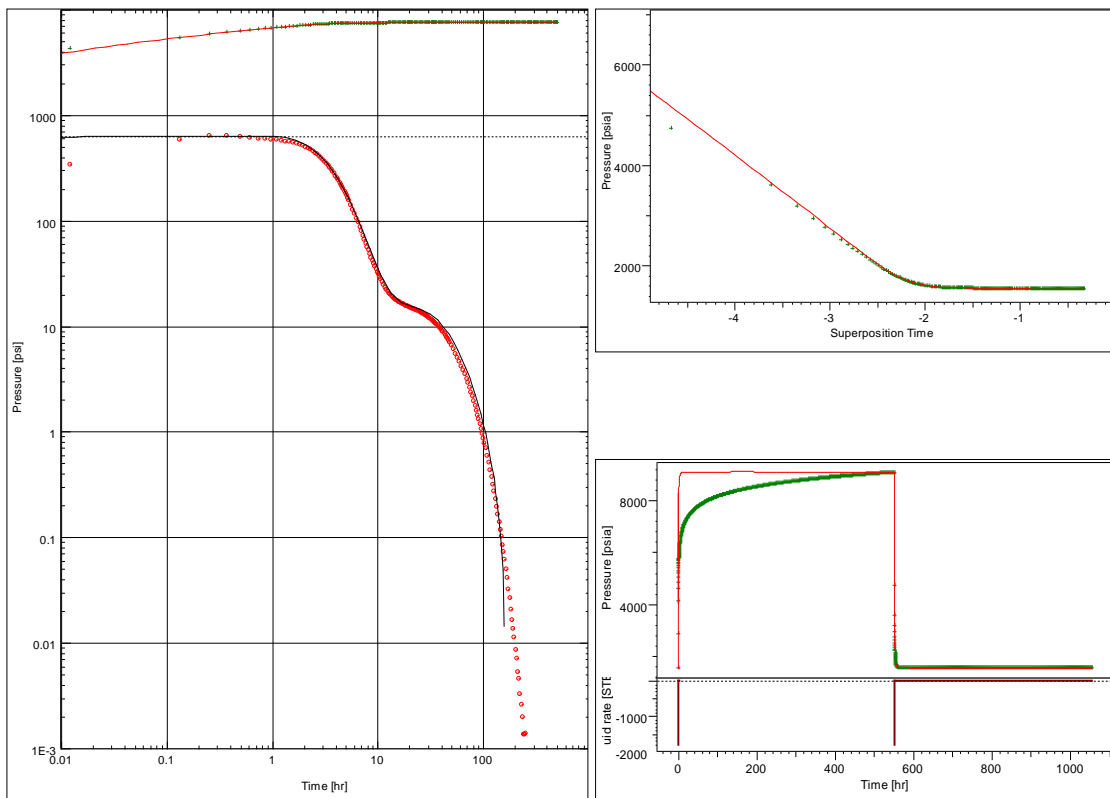


Figure D- 13: Log-log, semi-log and history plot for 51 days polymer injection with $C = 1.25 \text{ kg/m}^3$

Effect of shear-thinning fluids

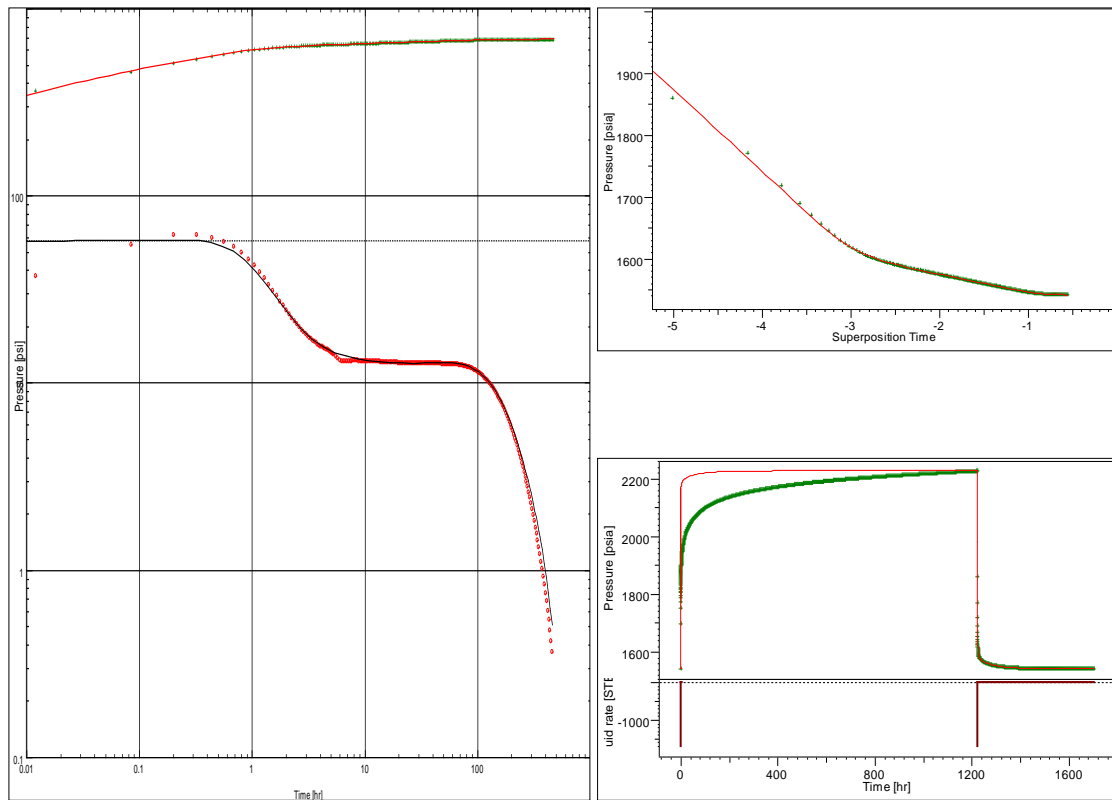


Figure D- 14: Log-log, semi-log and history plot for 51 days shear-thinning polymer injection with $C = 0.5 \text{ kg/m}^3$

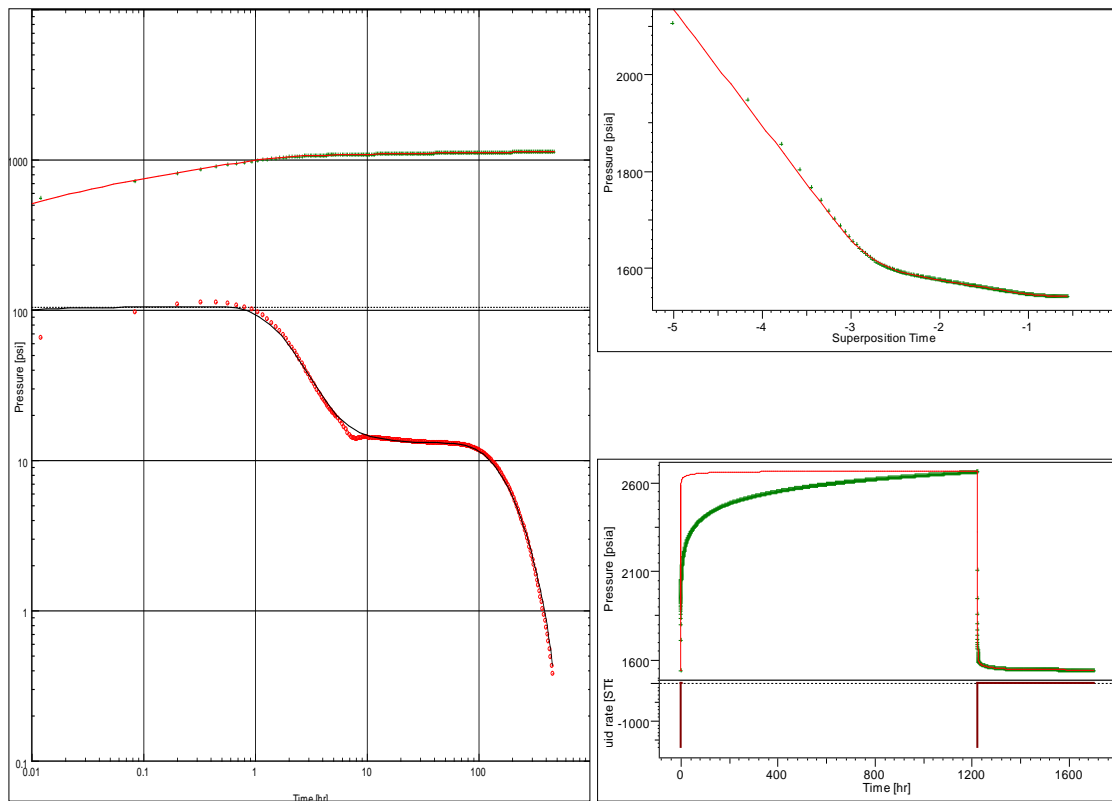


Figure D- 15: Log-log, semi-log and history plot for 51 days shear-thinning polymer injection with $C = 0.75 \text{ kg/m}^3$

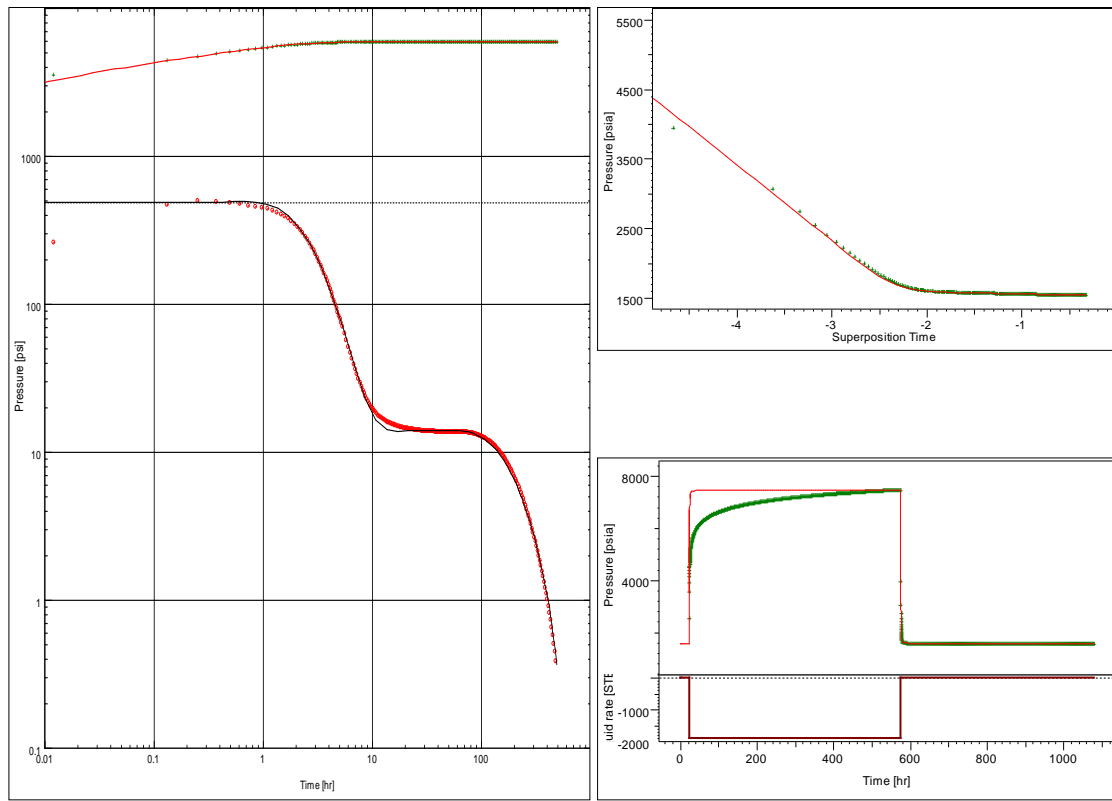


Figure D- 16: Log-log, semi-log and history plot for 51 days shear-thinning polymer injection with $C = 1.0 \text{ kg/m}^3$

Appendix E: Rheology of Polymer Solutions

In the laboratory, the measured viscosity of this polymer solution follows the power law model.

By plotting the shear rate and viscosity on the logarithmic scales, the parameters K and n in power law correlation can be determined. The slope and intercept are an indicative of exponent n and K.

The value of n is equal to one minus slope and k is equal 10 to the value of the intercept of the log-log plot as shown in Figure E- 1. It appears n is equal to 0.71 and K is equal to 32.25 cP.s^{-0.29}.

$$\mu_{app} = K\gamma^{n-1}$$

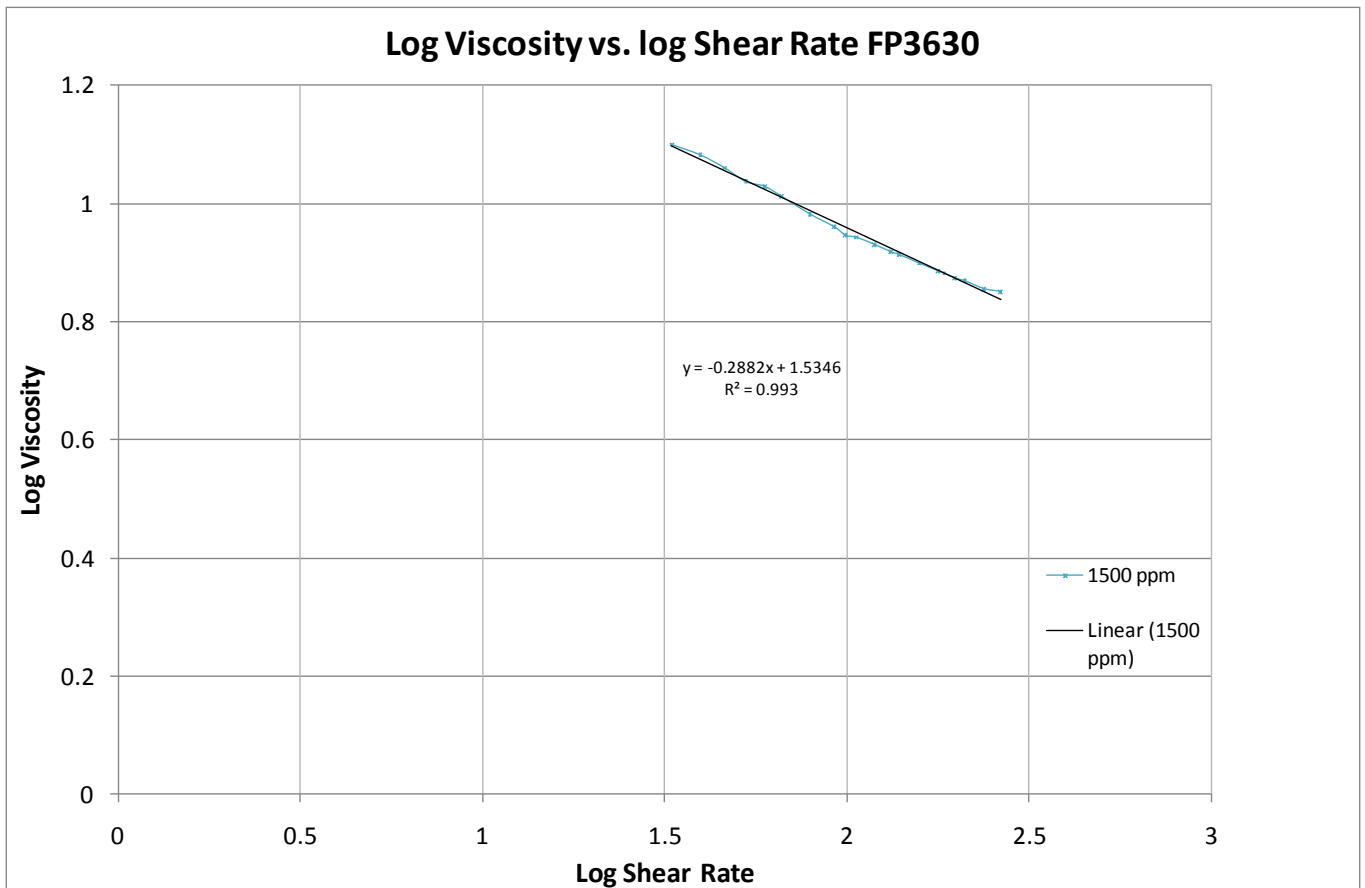


Figure E- 1: Log-log plot of polymer shear rate and viscosity